



DEGREE PROJECT IN VEHICLE ENGINEERING,
SECOND CYCLE, 30 CREDITS
STOCKHOLM, SWEDEN 2021

Performance comparison between reciprocating and scroll compressor heat pumps with R600a refrigerant

CHRISTOFER KRONSTRÖM

Abstract

A performance comparison of heat pumps using a scroll (Sanden) and a reciprocating (Bitzer) compressor was conducted experimentally. The refrigerant used was R600a (isobutane). The heat pump components were evaluated performance-wise through: volumetric and isentropic efficiency of the compressors; the UA-value of the condensers and evaporators; sensible enthalpy differences between the liquid and the suction line in the internal heat exchanger; and overall heat pump system comparison as the coefficient of performance.

The Bitzer heat pump had existing measuring devices and equipment installed, and it was already filled with refrigerant. The Sanden heat pump required installation of equipment and measuring devices and a refrigerant refill. The refrigerant charge was decided according to the criteria of the lowest compressor speed, which had an effect of overcharge for higher speeds. The measurements included the temperature of water and refrigerant, pressure of the refrigerant, water volume flow, and compressor power. The heat pumps performances were then evaluated based on these parameters.

The Sanden compressor showed higher volumetric efficiency than the Bitzer compressor, for the two lower (out of three) speeds of the compressor. The isentropic efficiency of the Bitzer compressor proved to be higher for all pressure ratios out of the three speeds respectively. The condenser in the Bitzer heat pump showed proper UA-values based on the temperature differences between refrigerant and heat sink. The UA-values of the Sanden heat pump condenser did not increase with compressor speed which then gave a larger temperature difference between refrigerant and heat sink, for the two higher compressor speeds. The evaporators had a similar issue with the temperature difference between refrigerant and heat source, which also showed on the UA-values. The internal heat exchanger in the Bitzer heat pump had a larger sensible enthalpy difference on the suction side compared to the liquid side, when condenser subcooling was low, indicating that some fraction of refrigerant was being condensed instead. The Sanden heat pump instead had higher condenser subcooling and the sensible enthalpy difference showed to be very low in the internal heat exchanger. Finally, the coefficient of performance showed to be slightly higher in the Bitzer heat pump for almost all evaluated condensation and evaporation temperatures.

Keywords: Heat pump, R600a, isobutane, scroll compressor, reciprocating compressor, piston compressor

Sammanfattning

En jämförelse av prestandan för två värmepumpar, en med scroll- (Sanden) och en med kolvkompressor (Bitzer) har gjorts. Köldmedlet som användes var R600a (isobutan). Komponenterna och hur deras prestanda blev utvärderad följer här: kompressorernas volymetriska och isentropisk verkningsgrad; kondensorns och förångarens UA-värden; den sensibla entalpiskillnaden mellan gas- och vätskeledning i den interna värmeväxlaren; en övergripande jämförelse av värmepumparna i form av deras värmefaktor.

Värmepumpen med Bitzerkompressor utvärderades med befintliga komponenter och mätutrustning, och en redan fylld mängd köldmedium. Värmepumpen med Sandenkompressor installerades med mätutrustning och komponenter, och fylldes med köldmedium. Mängden köldmedium bestämdes utifrån kriterier för det lägsta varvtalet på kompressorn, vilket visade sig ge en för stor mängd köldmedium vid de högre varvtalen. Mätningarna inkluderade temperatur på vatten och köldmedium, köldmediets tryck, vattnets volymflöde samt kompressorns effektbehov. Prestandan för värmepumparna är sedan utvärderad utifrån dessa data.

Sandenkompressorn visade en högre volymetrisk verkningsgrad för de två lägre (av tre) hastigheterna utvärderade i experimenten, jämfört med Bitzer. Den isentropiska verkningsgraden var högre i Bitzerkompressorn för samtliga tryckförhållanden för de tre respektive hastigheterna. Kondensorn i Bitzervärmepumpen uppvisade goda UA-värden, baserat på temperaturskillnaderna mellan köldmedium och värmesänka. Kondensorn i Sandenvärmepumpen visade ingen förbättring av UA-värden när kompressorns hastighet ökade, vilket i sin tur gav upphov till stora temperaturskillnader mellan köldmediet och värmesänkan. Förångarna i båda värmepumparna uppvisade liknande problem med höga temperaturskillnader mellan värmekälla och köldmedium, vilket även deras UA-värden visade. Den interna värmeväxlaren i Bitzervärmepumpen visade större skillnad i den sensibla entalpin på sug- jämfört med vätskesidan, när underkylningen i kondensorn var låg, vilket indikerade på att en del av köldmediet istället kondenserade. I Sandenvärmepumpen var kondensorns underkylning högre vilket då uppvisade en liten skillnad i den sensibla entalpin mellan de båda sidorna. Slutligen så visade Bitzervärmepumpen en något högre värmefaktor än Sandenvärmepumpen för nästan alla utvärderade kondenserings- och förångningstemperaturer.

Nyckelord: Värmepump, R600a, isobutan, scrollkompressor, kolvkompressor

Acknowledgement

I want to thank all the people that assisted me throughout my master thesis. Special thanks to the people involved in this project: Klas Andersson, Eric Granryd, Viktor Ölen, my examiner Björn Palm and last but not least my supervisor Jan-Erik Nowacki. Many thanks to you all for great discussions, for sharing your knowledge, and for visiting me during my work in the lab of Applied Thermodynamics and Refrigeration at KTH.

I also want to express gratitude to all the people that I got to know and had discussions with in the lab. Special thanks go out to Peter Hill and Albin Svensson, for always lending a helping hand, for which my experiments would have been impossible to conduct without.

Table of Contents

List of Figures

List of Tables

List of Abbreviations

1	Introduction	1
1.1	Background	1
1.2	Purpose	2
1.3	Scope	3
1.4	Limitations	3
2	Research Methodology	5
2.1	Experiment variables	5
2.2	Performance evaluation	6
2.3	Experiments	9
3	Implementation	11
3.1	Components	11
3.2	Measurement devices	13
3.3	Modifications	15
3.4	Preparatory work	15
4	Results	17
4.1	Compressor	17
4.2	Condenser performance	20
4.3	Evaporator performance	24
4.4	Internal heat exchanger	27
4.5	Coefficient of performance	28
4.5.1	Bitzer heat pump	28
4.5.2	Sanden heat pump	30
5	Discussion	32
5.1	Compressor	32
5.2	Condenser performance	34

5.3	Evaporator performance	35
5.4	Internal heat exchanger	36
5.5	Coefficient of performance	38
5.6	Future Work	40
6	Conclusion	41
	Bibliography	43
A	Components, equipment & measurement points	45
B	Temperatures in HEX	49
B.1	Bitzer	49
B.2	Sanden	53
C	Temperature change with different water mass flow condenser	55
D	Superheat and subcooling	57
E	Heating, cooling & compressor power	58

List of Figures

3.1	Drawings of the compressors.	12
a	Bitzer semi-hermetic reciprocating compressor	12
b	Sanden scroll compressor SHS33	12
3.2	Measurement locations and equipment in the heat pump systems.	14
a	Locations.	14
b	Equipment (<i>Sanden in italic</i>).	14
4.1	Isentropic efficiency at different speeds of the compressors. . . .	18
a	Bitzer compressor.	18
b	Sanden compressor.	18
4.2	Volumetric efficiency at different speeds of the compressors. . .	19
a	Bitzer compressor.	19
b	Sanden compressor.	19
4.3	UA-value of the condensers used in the two heat pumps.	21
a	Bitzer condenser (SWEP B25THx40).	21
b	Sanden condenser (Alfa Laval CB24).	21
4.4	UA-value of the Sanden condenser with temperature lift.	22
4.5	Inlet/outlet temperature difference in condenser and subcooling.	23
a	Bitzer condenser (SWEP B25THx40).	23
b	Sanden condenser (Alfa Laval CB24).	23
4.6	UA-value of the evaporators used in the two heat pumps	25
a	Bitzer evaporator (SWEP F85Hx20/1P-NC-M).	25
b	Sanden evaporator (Alfa Laval CB24).	25
4.7	Inlet/outlet temperature difference in evaporator and superheating.	26
a	Bitzer evaporator (SWEP F85Hx20/1P-NC-M).	26
b	Sanden evaporator (Alfa Laval CB24).	26
4.8	Enthalpy balance of the internal heat exchanger.	27
a	Bitzer Internal heat exchanger (SWEP B10THx30).	27
b	Sanden internal heat exchanger (Pentaprop condenser). . .	27
4.9	Coefficient of performance of the Bitzer heat pump.	29
a	Compressor speed 25 Hz.	29
b	Compressor speed 50 Hz.	29
c	Compressor speed 75 Hz.	29

4.10	Coefficient of performance of the Sanden heat pump.	31
a	Compressor speed 2000 rpm.	31
b	Compressor speed 4000 rpm.	31
c	Compressor speed 6000 rpm.	31
5.1	Enthalpy balance of the internal heat exchanger [%]	37
a	Bitzer Internal heat exchanger (SWEP B10THx30))	37
b	Sanden internal heat exchanger (Pentaprop condenser)	37
5.2	Carnot efficiency for refrigeration.	39
a	Bitzer heat pump	39
b	Sanden heat pump	39
A.1	Bitzer heat pump	45
A.2	Measurement points on water circuit	46
A.3	Measurement equipment	47
A.4	Sanden heat pump	48
B.1	Temperature profile in the condenser (length x only estimated and not calculated)	49
B.2	Temperature profile in the evaporator (length x only estimated)	50
B.3	Temperature differences in condenser.	50
B.4	Temperature differences in evaporator.	51
B.5	Example of temperatures when the sensible enthalpy is equal for liquid/suction side.	51
B.6	Example of temperatures when sensible enthalpy is not equal for liquid/suction side.	52
B.7	Temperature profile in the condenser (length x only estimated).	53
B.8	Temperature profile in the evaporator (length x only estimated).	53
B.9	Temperature differences in condenser.	54
B.10	Temperature differences in evaporator.	54
C.1	Condensation temperature change with water mass flow, Sanden heat pump experiment.	55
C.2	Temperature profile in condenser with different water flows (length x only estimated).	56
D.1	Superheat & subcooling in experiments.	57
a	Bitzer heat pump.	57
b	Sanden heat pump.	57

List of Tables

2.1	Independent and dependent variables in the experiments.	5
E.1	Heating, cooling & compressor power	59
a	Sanden heat pump.	59
b	Bitzer heat pump.	59

List of Abbreviations

COP Coefficient Of Performance.

GWP Global Warming Potential.

HFC Hydrofluorocarbon.

LMTD Logarithmic Mean Temperature Difference.

ODP Ozone Depletion Potential.

Chapter 1

Introduction

Increasing efficiency is an ever important goal in many fields, especially in the field of energy. Lowering the total emission of greenhouse gases into the atmosphere, is today an equally important goal. In heat pumps, using more efficient compressors, heat exchangers, and expansion valves, in combination with natural refrigerants, comply especially well with the goals above. A heat pump is an efficient way of utilizing a source at low temperature to be given off at a higher temperature.

Two well-known compressor types are the scroll- and reciprocating piston type compressors. Both are suitable for many different applications. In order to establish the advantages and disadvantages of using each technique, their performances need to be evaluated.

1.1 Background

There are different types of compressors used for heat pump and air conditioning applications. The optimal compressor type depends mainly on the required size (kW) of the heat pump, and the required pressure ratio (outlet and inlet). For refrigerant flows below 10 l/s, commonly reciprocating, scroll, or rotary compressors are used [1].

A scroll compressor has fewer moving parts than a reciprocating one, and emits less noise. They often reach higher volumetric efficiency, having no dead space left after compression. However, a scroll compressor has a built-in volume ratio instead. Scrolls are less sensitive to liquid entering the compressor. [1, 2]

The system charge is important for the performance of a heat pump and it was found that an undercharge of 25 % gave a decrease in the cooling capacity of 20 % and a 15 % decrease in energy efficiency [3]. Another study comparing a reciprocating compressor with a scroll compressor, showed that overcharge had even greater impact on the performance than undercharge. The same study showed that the superheat in the evaporator decreased while increasing the

charge. At the same time the subcooling after the condenser increased using a larger charge. Subcooling and superheat were also found to be good indicators of the optimal charge. Moreover, the study found the scroll compressor to have equal or greater cooling capacity and Coefficient Of Performance (COP) as compared to the reciprocating compressor. [4]

The volumetric efficiency of a scroll compressor is generally less sensitive, than a reciprocating compressor, to a high pressure ratio. For low to moderate pressure ratios, the scroll compressor can also achieve a higher isentropic efficiency than the reciprocating one. [1]

Natural refrigerants like R290 and R600a are hydrocarbons, containing no fluorine or chlorine, resulting in no Ozone Depletion Potential (ODP) and a very low Global Warming Potential (GWP). They are low-poisonous, however flammable. Both these refrigerants are important substitutes when phasing out Hydrofluorocarbon (HFC). A reduction of CO₂ equivalent to a level of 35 MT should be made in Europe by 2030. That is a reduction of 60 % compared to levels in 2005, as stated by [5]. A common use today for R600a is in refrigerators or other small systems due to the limited amount of charge needed - below 150 grams [6]. Reducing the charge of the refrigerant was one of the prime aspects evaluated in [7].

In [7] a heat pump with a scroll compressor and isobutane as refrigerant was evaluated. The results showed an isentropic efficiency between 50-73 %, a volumetric efficiency between 86-94 %, and a COP for heating between 3.7 and 11. A study [8] which conducted simulations on the performance of pure hydrocarbon refrigerants, found R600a to achieve higher COP compared to R134a and R290. This was for refrigeration purposes with evaporation temperature range between -30 to 0 °C and condensation temperature between 30-50 °C.

1.2 Purpose

A comparison between the two compressor types in terms of multiple performance aspects was not found by the author at the time of writing this thesis. Also few articles regarding the scroll compressor that uses R600a as refrigerant were found. This thesis may thus contribute to the research field. Research that involves natural refrigerants in heat pumps is vital, since there is and probably will remain an upper limit on the charge for these flammable refrigerants.

1.3 Scope

This thesis work experimentally compared the performance of two heat pumps with different compressor types, both operated with a natural refrigerant (R600a): one used a scroll (Sanden) and the other a reciprocating piston (Bitzer) compressor. The units were meant for applications with high-temperature heat pumping. The scroll compressor heat pump was intended for a minimum charge of refrigerant, while this was not an issue for the reciprocating piston, which was intended for larger cooling capacity. The eventual purpose for both heat pumps is to be used as dedicated mechanical subcooling for a larger heat pump, also known as economizer heat pumps. Various performance aspects were measured for an overall system evaluation. The research questions are presented here.

Research Questions

1. What is the difference in performance between the heat pump systems?
The aforementioned difference being measured in terms of:
 - the compressor efficiency,
 - and the overall heat pump performance, COP.
2. How do the different heat exchangers perform in the two units? Which includes:
 - the evaporator,
 - the condenser,
 - and the internal heat exchanger.

1.4 Limitations

The refrigerant evaluated is only R600a, and evaluations will only be for one amount of charge. The heat sink- and heat source fluid is water, thus the temperature for the outgoing water at the heat source is limited to above the freezing point (0 °C) temperatures. Pressures were only measured at a few places. Thus, pressure losses occurring in some components could not be accounted for. Temperatures were measured on pipe surfaces at some points, where considered important though, they were measured using capillary tubes welded into the

pipes. There are different distances of pipe (insulated in most cases) before and after the temperature measuring points. Heat conduction in the pipe material or heat losses to the are not accounted for.

Chapter 2

Research Methodology

The methodology is divided into three sections which describe and motivate the methodology used for collecting the data in the experiments. First, a section containing the independent variables obtained from the experiments. The second section is where the governing equations are presented, which as input has the independent variables and as output the dependent variables. The third section describes the experimental procedure.

2.1 Experiment variables

In the following section the variables in the experiments are presented, which are listed in table 2.1. There are independent variables that will change with how and where the measurements are made. Dependent variables are obtained from calculations using the measured independent variables.

Table 2.1: Independent and dependent variables in the experiments.

Dependent	Independent
Heating & Cooling capacity	Water temperature & flow rate
Evaporator performance	Refrigerant low pressure, water flow rate & heat source temperatures
Condenser performance	Refrigerant high pressure, water flow rate & heat sink temperatures
Internal heat exchanger performance	Refrigerant inlet and outlet temperatures, low & high pressure
Compressor performance	Refrigerant low & high pressure, compressor electric power, speed, inlet and outlet temperatures
COP	Compressor electric power, water temperature & flow rate

The refrigerant pressures, water flows, and temperatures (for both the refrigerant and water) were obtained with measurement devices (further shown in Figure 3.2). The remaining variables were obtained via calculations.

Thermocouples measuring the water and refrigerant temperatures were connected to external ports connecting to the data acquisition unit. The external port only allowed for a certain number of connected thermocouples. The number of ports constraint means that the temperatures could only be measured once between each component. A better solution to account for heat losses in pipes would be to measure the temperatures at two places between every component. For instance, measuring the temperature first immediately after the compressor outlet and then again close to the condenser inlet. Installing another external port and then re-programming the software could not be achieved within the time frame of the thesis. However, insulation of all pipes was made thoroughly to minimize the losses between the components.

There were three transducers measuring the refrigerant pressures. The limitation to three was again the availability of ports in the data acquisition unit. The most desired pressures to measure were of course condensation and evaporation inside the heat exchangers. Pressure measurements are however difficult to perform inside heat exchangers, and pressures are not constant throughout these components either. Thus, the pressures were taken as the measured pressure in the inlet or the outlet of the evaporator or condenser. To have measured the pressures both at the inlets and outlets would of course be more ideal. However, a third pressure transducer was used for mobile measurements and was moved to different locations between the experiments. It was mainly placed on the opposite side of the fixed pressure transducer, to quantify the pressure drop in the condenser and evaporator. The pressure drops were then found to be small and that they could be neglected.

2.2 Performance evaluation

The performance was evaluated with the equations presented in this section. Furthermore, the performance was also compared with unpublished and published experiments made on both heat pumps [7].

The calculations for the heat delivered (\dot{Q}_1) and absorbed (\dot{Q}_2) by the heat pump are based on the measurements made from the water side. The relation used for

the heating- and cooling capacity is given in equation 2.1

$$\dot{Q} = \dot{V} \rho C_p \Delta T \quad (2.1)$$

where ρ and C_p is the density and specific heat of the water respectively, at the corresponding temperature where the volume flow (\dot{V}) was measured. ΔT is the temperature difference of the water at the inlet and outlet of the evaporator and condenser.

Using a heat balance, the mass flow of the refrigerant (\dot{m}_{ref}) could be calculated. The relation for the heat exchange on the refrigerant side is shown in equation 2.2.

$$\dot{Q} = \dot{m}_{ref} \Delta h \quad (2.2)$$

The enthalpy difference Δh was derived from the pressures and temperatures.

The performance of any heat exchanger in the system is dependent on the amount of heat transferred between the two media flows. This can be determined as the product of the overall heat transfer coefficient (U), the heat transfer area (A) and the Logarithmic Mean Temperature Difference (LMTD) or ϑ_m . The UA-value of a heat exchanger can thus be determined by using equation 2.3.

$$\dot{Q} = UA \vartheta_m \quad (2.3)$$

The LMTD ϑ_m can here be calculated according to equation 2.4. This requires knowing the temperature difference of the incoming (ϑ_{in}) and outgoing (ϑ_{out}) fluids in the heat exchanger. The difference considered is between the temperature of the inlet or outlet of the water compared with the refrigerants condensation or evaporation temperature.

$$\vartheta_m = \frac{\vartheta_{in} - \vartheta_{out}}{\ln\left(\frac{\vartheta_{in}}{\vartheta_{out}}\right)} \quad (2.4)$$

With the heat transfer in the evaporator and condenser and with the measured electric power going to the compressor \dot{E}_k , two COP's can be calculated using equation 2.5.

$$COP = \frac{\dot{Q}}{\dot{E}_k} \quad (2.5)$$

If the delivered heat is used in 2.5, COP_1 is defined while if the absorbed heat is used instead, COP_2 is defined. The maximum COP that can be achieved for a

heat pump or a cooling machine is defined as the Carnot COP, here shown for cooling (COP_{2C}) in equation 2.6.

$$COP_{2C} = \frac{T_2}{T_1 - T_2} \quad (2.6)$$

Where T_1 and T_2 are the refrigerant condensation and evaporation temperatures respectively. With equations 2.5 and 2.6, the Carnot efficiency for refrigeration (η_{Ct2}) can be determined, as seen in equation 2.7.

$$\eta_{Ct2} = \frac{COP_2}{COP_{2C}} \quad (2.7)$$

The Carnot efficiency for refrigeration (η_{Ct2}) is in practice the one of interest. This is due to that any electric heater achieves a COP_1 equal to one, and hence a non-zero Carnot efficiency for heating (η_{Ct1}). The Carnot efficiency is normally between 0.4 and 0.6 for a vapor compression cycle [1].

Neglecting other heat exchanges with the surrounding gives $COP_1 = COP_2 + 1$, and combining this with equations 2.6 and 2.7, the COP for heating can then be expressed as seen in equation 2.8.

$$COP_1 = 1 + \eta_{Ct2} \left(\frac{T_2}{T_1 - T_2} \right) \quad (2.8)$$

The performance of the compressor is often evaluated in means of volumetric, adiabatic, and isentropic efficiency. The volumetric efficiency (η_s) is calculated with equation 2.9.

$$\eta_s = \frac{\dot{V}_2}{\dot{V}_S}, \quad \dot{V}_2 = \dot{m}_{ref} \nu_{2k} \quad (2.9)$$

where \dot{V}_S is the theoretical swept volume, for the Bitzer compressor $\dot{V}_S = 22.7 \text{ m}^3/\text{h}$ at 50 Hz, for the Sanden compressor $\dot{V}_S = 3.96 \text{ m}^3/\text{h}$ at 2000 rpm. \dot{V}_2 is the actual volumetric flow rate, calculated using the mass flow and the specific volume ν_{2k} of the refrigerant entering the compressor.

The adiabatic efficiency (η_{ad}) is the ratio between an isentropic compression and the actual one. This is measured based on the enthalpies at the entry (h_b) and exit (h_c) of the compressor, compared to the corresponding enthalpy h_{cis} for an isentropic compression and is shown in equation 2.10.

$$\eta_{ad} = \frac{h_{cis} - h_b}{h_c - h_b} \quad (2.10)$$

The total isentropic efficiency (η_{isen}) is a comparison between the measured electric power for the compressor (\dot{E}_k) and the isentropic compression power as shown in equation 2.11.

$$\eta_{isen} = \frac{\dot{m}_{ref}(h_{cis} - h_b)}{\dot{E}_k} \quad (2.11)$$

If the compressor is completely isolated to the surroundings (no heat losses) the adiabatic and isentropic efficiency is equal. The isentropic efficiency is in practice the one of interest.

2.3 Experiments

The experimental procedure for both heat pumps with the different compressor types is presented here.

Bitzer The heat pump was evaluated for three different compressor speeds 25, 50 and 75 Hz. 50 Hz is the normal speed (grid frequency) for the compressor when it is running without altering the frequency. At 50 Hz tests were made for three different condensation temperatures 50, 60 and 70 °C. For this heat pump, these temperatures also coincided with the temperatures of the outlet water in the heat sink, which was an indication of a well-performing condenser. In addition, the heat pump was also evaluated at compressor speeds of 25 and 75 Hz, to compare with the 50 Hz speed. This was done for two condensation temperatures, 50 and 70 °C. For each condensation temperature, tests were made for three evaporation temperatures. The temperatures for condensation and evaporation were regulated with PID controllers (further described in section 3.1). The water flow was varied between 0.17-0.66 l/s for the different measurement points. The variation was set to get a sufficient temperature difference of the water between inlet and outlet in the heat source and sink. Having a small temperature difference results in higher uncertainties, for that reason a minimum temperature difference of around 3 K was chosen. The condensation pressure was measured at the inlet of the condenser. The evaporation pressure was measured between the internal heat exchanger and the inlet to the compressor (point B in Figure 3.2a). Potential pressure losses in the internal heat exchanger will cause this pressure to be lower than the actual evaporation pressure. Due to that, the mass flow was determined from the heat balance in the condenser instead. However, the performance of the evaporator and the in-

ternal heat exchanger was evaluated with the pressure measured in point B. The expansion valve was regulated with a PID controller, and was set to maintain a superheat of 5 K after the evaporator. Each test run was maintained stable for a minimum of 600 seconds. The total energy consumption was measured during this time and was used to calculate the average power consumption.

This average power consumption also included auxiliary equipment for the compressor such as an oil heater and warning for oil levels. The frequency inverter that controls the speed of the compressor was also included in the average power consumption. The inverter was bypassed for some tests running at 50 Hz to estimate its power consumption and its effect on isentropic efficiency.

Sanden This heat pump was evaluated for three different speeds, 2000, 4000 and 6000 rpm. It was evaluated for three different temperatures of the outlet water in the heat sink, 50, 60 and 70 °C. In this case, these temperatures did not fully coincide with the condensation temperatures of the refrigerant. Meaning there was sometimes a large temperature difference between the condensing temperature and the outlet water temperature in the condenser. Having a lower mass flow of the water through the condenser made this temperature difference smaller and thereby decreasing the condensation temperature (further details in Appendix C). The water flow was varied between 0.065-0.63 l/s for the different measurement points. The variation was made to maintain the water temperature difference above 3 K (as described in the Bitzer experiments, section 2.3), and at the same time maintain sufficient flow to make sure that the LMTD-method was valid. The condensation pressure was measured at the condenser inlet. The evaporation pressure was measured at the evaporator outlet. For each heat sink outlet temperature, tests were made for three evaporation temperatures, 15, 25 and 35 °C. The superheating was set between 1-2 K which however resulted in a measured superheat between 2-6 K. Time for each test run and power measurements were done in the same way as for the Bitzer heat pump. Power measurements only included the compressor requirement and no auxiliary equipment.

Chapter 3

Implementation

In this chapter, the systematic approach adopted throughout this thesis work is presented. This consisted of identifying the system requirements, listed here as R1-R4, and meeting them. This chapter provides a more elaborate description of how the requirements were met.

- R1** Utilize existing experimental facility and components to the greatest extent possible to avoid time-consuming research and re-construction.
- R2** Importance of securing the phase of the refrigerant through the condenser and evaporator. I.e pure liquid out of the condenser and pure vapor out of the evaporator.
- R3** Minimize the negative impact on the environment, it should be reduced to the extent possible.
- R4** In order to be run commercially and experimented on, the compressor should be approved for natural refrigerants.

Said requirements impact how the experimental facility was modified and set up. A more detailed description of the experimental facility is provided here, in terms of its components and sensors. Moreover, the modifications made to the facility that were needed to meet the system requirements are also presented. Almost all of the components and measurement devices used for the experiment were available for this study and did not have to be ordered. Therefore, meeting the requirement R1. Both heat pumps were running with R600a (isobutane) as refrigerant, which is better from an environmental point of view, meeting requirement R3.

3.1 Components

This section lists the components that were used in the experiments. The water circuit was common for the two heat pumps and is described first.

The heat source and heat sink medium is water for the two heat pumps. For circulation of the water to the heat sink a Calio 32-120 pump is used, for the heat source a Wilo Stratos 30/1-12 pump is used. The temperatures of the inlet water to the evaporator and the outlet water of the condenser are controlled with PID regulators. These are of the brand Eurotherm 2408 for the condenser and Eurotherm 3508 for the evaporator. The PID controllers regulate the temperature by the use of three-way valves (M in Figure 3.2a), of type Esbe 12500100 62p. A large tank with around one cubic meter of water is used to both transfer heat from the condenser water and also add heat to the evaporator water. The specific heat pump components are described below.

Bitzer This heat pump is using a Bitzer semi-hermetic compressor (Figure 3.1a) model 4EESP-4Z-40S, meeting requirement R4. The speed of the compressor is regulated with a frequency inverter, Eurotherm 650 series. The expansion valve is a Carel EVD evolution which is of the electronic type. This regulates the superheat by measuring the pressure and temperature of the refrigerant going out of the evaporator. The evaporator heat exchanger is a SWEP F85Hx20/1P-NC-M, with a heat transfer area of 1.080 m². The condenser is a SWEP B25THx40, with a heat transfer area of 2.394 m². There is an internal heat exchanger from SWEP model B10THx30/1P-SC-M, for additional superheating and subcooling of the refrigerant.

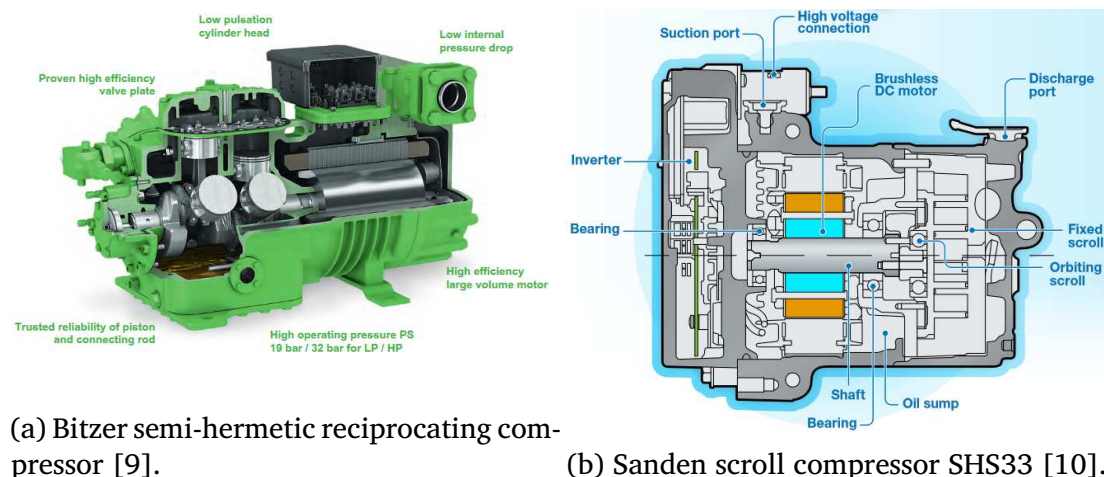


Figure 3.1: Drawings of the compressors.

Sanden The heat pump is using a Sanden SHS33 scroll compressor (Figure 3.1b) which is normally used for the air conditioning unit in electric vehicles. The speed of the compressor is regulated with a device that was custom made

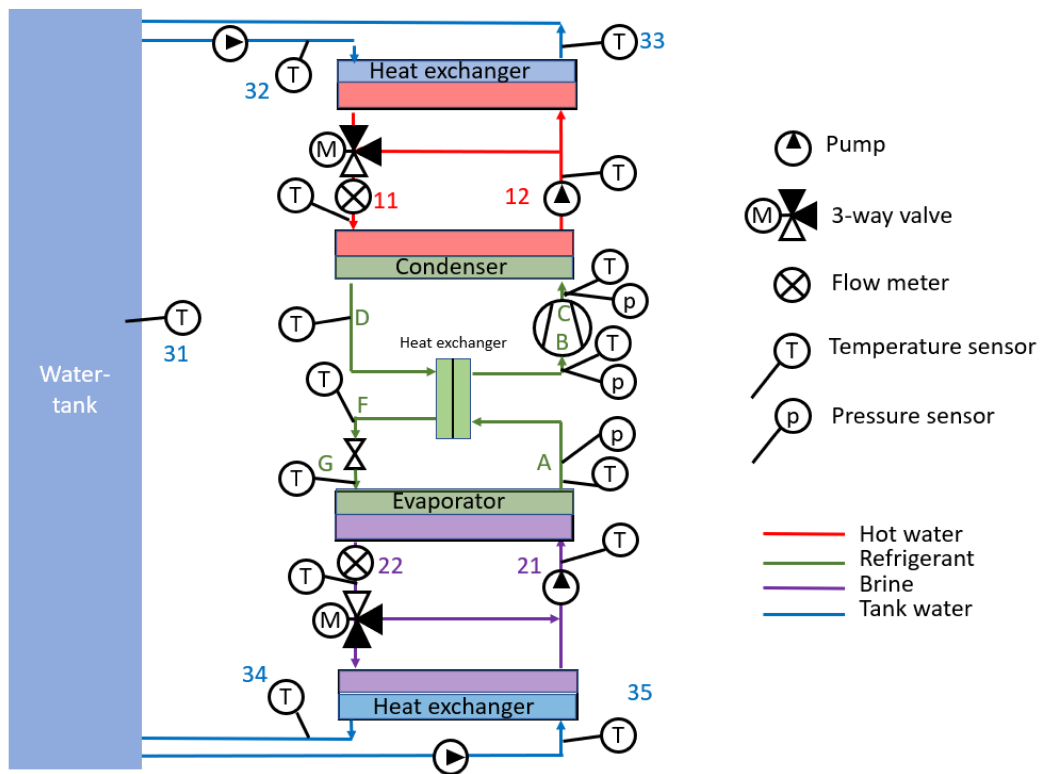
for this compressor. The condenser and evaporator is from Alfa Laval, model CB24. The internal volume of the condenser is 340 cm^3 and the evaporator 380 cm^3 . The internal heat exchanger is a Pentaprop condenser with 31 plates. Two expansion valves are installed in parallel in the circuit. One is meant for better control of the lower flows, the other for higher flows, meaning only one is active at a time. The expansion valve is a Carel EVD evolution, of the electronic type which regulates with the pressure and temperature after the evaporator. Experiments later showed that only the smaller expansion valve was necessary for all the experiments. There are three sight glasses installed in the refrigerant loop. These are located after the condenser, before the expansion valve and one after the evaporator.

The components in the Sanden heat pump have been selected to keep the charge of the refrigerant R600a below 150 grams, with the exception of the internal heat exchanger. This heat exchanger is used as a temporary solution awaiting the manufacturing of a more well-adopted internal heat exchanger.

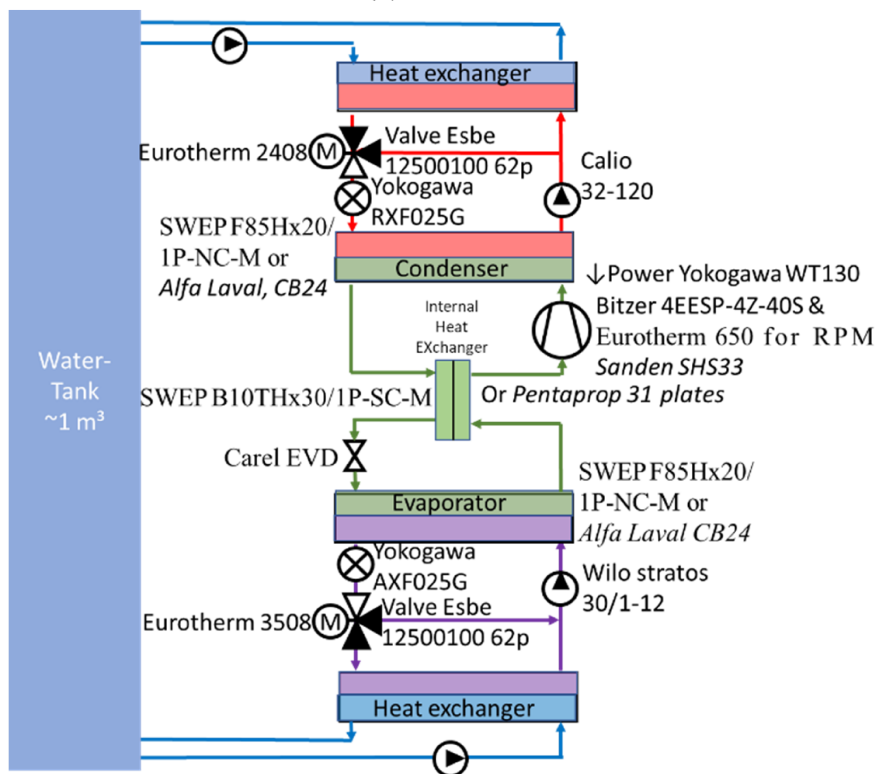
3.2 Measurement devices

The following section describes the equipment used for measurement. Most equipment is used for both heat pumps, whereas the pressures are measured with different devices.

The water flows are measured using a Yokogawa RXF025G and AXF025G, for the flows V_{12} and V_{21} respectively. The outputs from the measurement devices are then read by two acquisition units. Agilent 34972A for temperatures and pressure P_A , Agilent 34970A for pressures P_B and P_C . The two acquisition units are then connected to a computer and analyzed with Agilent Vee Pro 9.2. The power delivered to the compressor is measured using a Yokogawa WT130 digital power meter. The locations of the measurements and equipment can be further seen in Figure 3.2.



(a) Locations.



(b) Equipment (*Sanden in italic*).

Figure 3.2: Measurement locations and equipment in the heat pump systems.

There are temperature measurements between each component of the system. Thermocouples used were of the T-type. Specific locations of the devices and measurement points on the actual two heat pump setups can be seen in Appendix A.

Bitzer The refrigerant pressure is measured using absolute pressure transmitters of the kind Yokogawa EJA510E, for both the low-and-high pressure side. The measurement of the pressure in the evaporator was initially measured in point B, later a pressure transducer Carel SPKT0021CO was also installed in point A. The pressure should ideally also be measured in between every component to account for the pressure loss occurring in them, namely the places D, F and G (although there is no connection for a pressure transducer at point G in the current configuration of the heat pump) seen in the Figure 3.2a.

Sanden The pressure is measured using pressure transducers of the kind Druck Unik 5000, for both the low-and-high pressure side. The pressure was measured in points A and C. Furthermore a third pressure transducer of the kind Carel SPKT0021CO was placed at different locations during the experiments to quantify pressure drops.

3.3 Modifications

The Sanden scroll compressor heat pump was first tested with 300 grams of refrigerant. The measurements showed very low heating- and cooling capacity, which indicated poor heat transfer in the condenser and evaporator. At this time the heat pump was not equipped with sight glasses to ensure pure liquid out of the condenser and pure vapor out of the evaporator. For this the heat pump was rebuilt with sight glasses, before and after the evaporator and also one after the condenser, thus fulfilling R2.

3.4 Preparatory work

Bitzer Measuring devices and equipment were already installed for this rig and it was previously filled with refrigerant.

Sanden The Sanden heat pump had been previously evaluated in [7], that construction however contained a different internal heat exchanger. In [7] there were problems, measuring of the compressor power. The measurement equipment needed to be re-installed for this rig, as well as a more calibrated refill of refrigerant. The refrigerant charge, in this case, is between 350-400 grams, which is considerably higher than the previous 120 grams of charge in the experiments on the previous construction [7]. The increase of charge was mainly due to the new larger internal heat exchanger.

The new charge was calibrated to achieve sufficient subcooling in the condenser at the lowest speed of the compressor. Having low charge meant that the refrigerant often did not even fully condense in the condenser. The amount of subcooling increases with an increase of the compressor speed, which is why the lowest speed is chosen for calibration. A sight glass after the condenser, showed that it was necessary to fill refrigerant until 4 to 6 K subcooling was reached, until the vapor bubbles disappeared in the sight glass. The subcooling was measured as the difference between the corresponding saturation temperature at the compressor outlet and the refrigerant temperature at the condenser outlet. A pressure drop in the condensor resulted in a measured subcooling that was larger than the actual one.

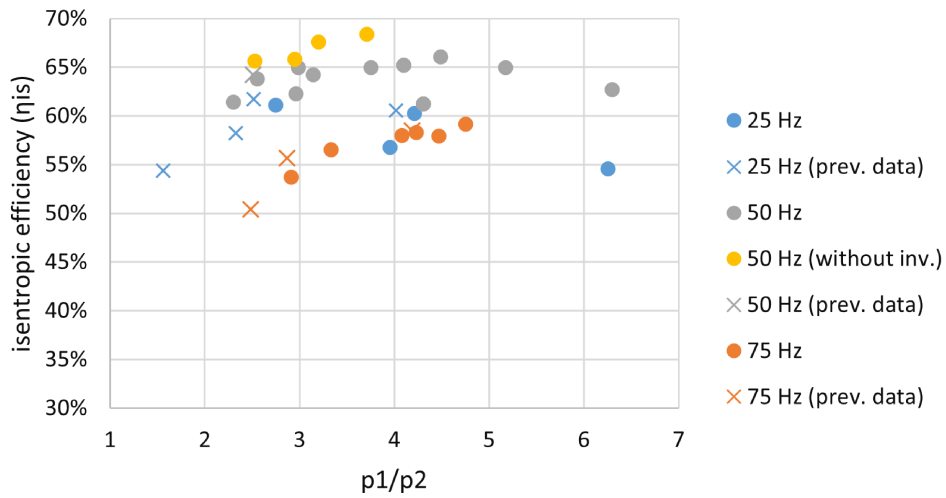
Chapter 4

Results

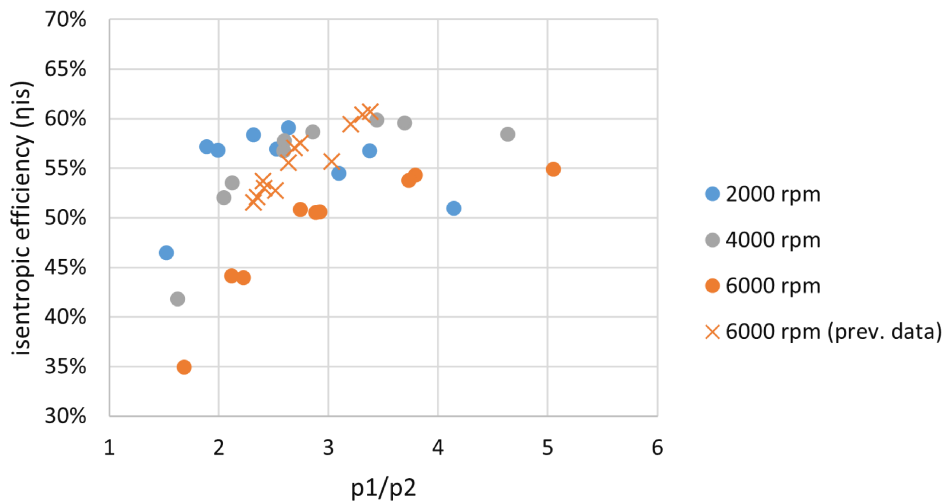
The following chapter shows the results of the experiments. Results are including the performance of the compressor, evaporator, condenser, internal heat exchanger and finally the overall performance of the heat pump, represented as e.g. the COP. Along with the data from the experiments made in this report, data from previous (unpublished) evaluations of the heat pumps will also be presented where appropriate. These unpublished data is then displayed with crosses instead of dots and described as "prev. data". An important consideration to have in mind in the analysis of the results is that the compressor speed, condensation temperature, and evaporation temperature differs between the two heat pumps.

4.1 Compressor

The isentropic efficiency of the compressors, depending on the pressure ratio for the different speeds can be seen in Figure 4.1. The Bitzer compressor generally has a higher isentropic efficiency when comparing the different speeds. Moreover, the Bitzer compressor (Figure 4.1a) has the overall highest isentropic efficiency when running the compressor at 50 Hz. The maximum point, using the inverter, is around 66 % at a pressure ratio of around 4.5. Running the heat pump directly without the frequency inverter increases the isentropic efficiency by 2-3 %. At 25 Hz the maximum efficiency appears at a pressure ratio between 2.5 and 4. A compressor speed of 75 Hz reaches the maximum efficiency of 59 % at the largest pressure ratio measured for that compressor speed, i.e., between 4 and 5.



(a) Bitzer compressor.

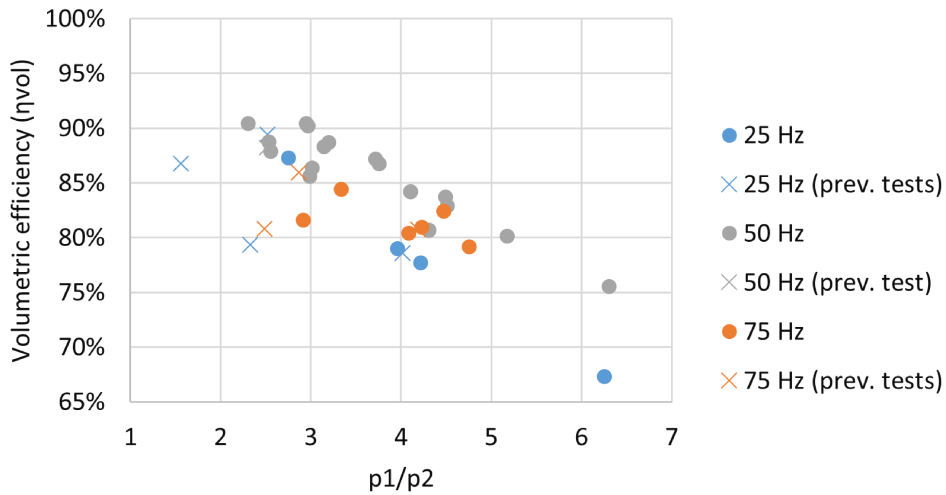


(b) Sanden compressor.

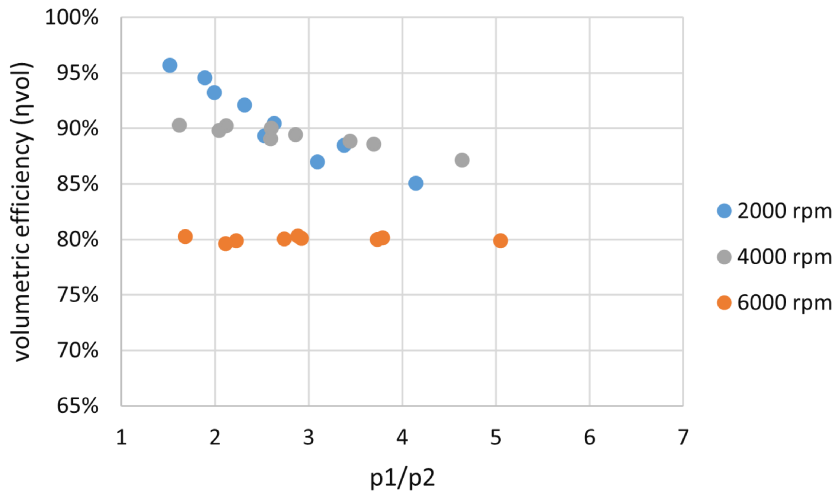
Figure 4.1: Isentropic efficiency at different speeds of the compressors.

The Sanden compressor (Figure 4.1b) reaches the highest efficiency at either 2000 or 4000 rpm, depending on the pressure ratio. For 2000 rpm about 59 % is achieved between 2-3 in pressure ratio and running at 4000 rpm about 60 % is achieved between 3-4 in pressure ratio. 6000 rpm has a maximum efficiency of around 55 % at the highest pressure ratio measured in the experiments. Previous tests made at 6000 rpm, showed greater values and also reached a higher isentropic efficiency than any of the tests made in this experiment.

The volumetric efficiency of the compressor as a function of the ratio between the condensation (p_1) and evaporation (p_2) pressure can be seen in Figure 4.2



(a) Bitzer compressor.



(b) Sanden compressor.

Figure 4.2: Volumetric efficiency at different speeds of the compressors.

The volumetric efficiency of the Bitzer compressor (Figure 4.2a) is overall decreasing with an increase in the pressure ratio. However, some anomalies can be observed for the speeds 25 and 75 Hz, both for the current experiment as well as for the previous tests made. The highest trend pattern can be seen at some of the points measured at 50 Hz compressor speed, where the highest volumetric efficiency is around 90 %. At pressure ratios below three, some results for a certain speed show different volumetric efficiency at the same pressure ratio. At the speeds of 50 and 75 Hz this shows at a pressure ratio around 3, for 25 Hz at a pressure ratio around 2.5. When the volumetric efficiency is higher for a certain pressure ratio, this is related to both a lower condensation and

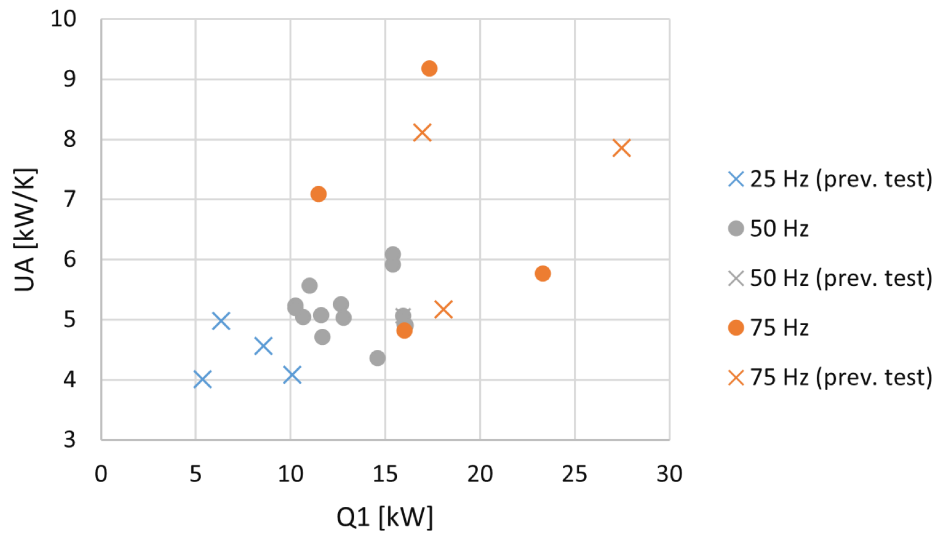
evaporation temperature, while the lower volumetric efficiency is for a higher condensation and evaporation temperature.

The Sanden compressor (Figure 4.2b) achieves its highest volumetric efficiency at 2000 rpm, around 96 % at the lowest pressure ratios. This trend continues at least for pressure ratios below 2.5, and above this where 4000 rpm is more efficient. Both 2000 and 4000 rpm have a decrease in efficiency as the pressure ratio increases, where 2000 rpm shows a larger decay than 4000. The speed 6000 rpm shows a different trend of being constant at 80 % and shows no change of the volumetric efficiency as the pressure ratio increases.

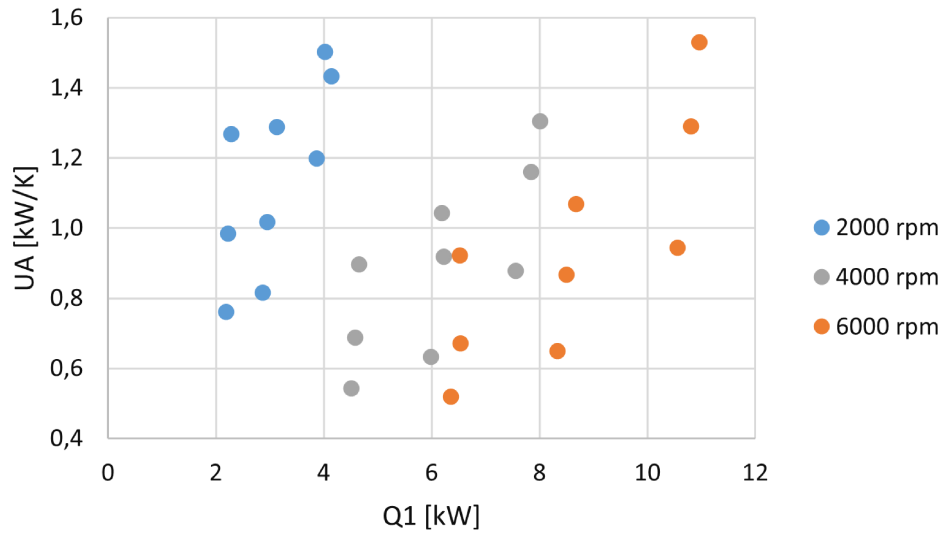
A comparison between the two compressors shows that the Bitzer has higher isentropic efficiency for the three speeds respectively. The Sanden compressor though, shows a higher volumetric efficiency for speeds between 2000 and 4000 rpm, as compared to the Bitzer compressor at the speeds 25 and 50 Hz. The Sanden compressor at 6000 rpm showed a lower volumetric efficiency than the Bitzer had at 75 Hz.

4.2 Condenser performance

The condenser from SWEP (Figure 4.3a) shows no clear trend for the UA-value at a compressor speed of 50 Hz, values vary from 4-6 kW/K. For compressor speed 75 Hz there are signs of two different patterns that increase with heating capacity, which reach up to 9 kW/K. However, the values above 7 kW/K are related to a very small temperature difference between the refrigerant and the outlet water (ϑ_{out}). This gives high uncertainty in the LMTD method and hence also the UA-values. The previous data evaluated on 25 Hz shows no trend for the UA with higher heating capacity, values vary from 4-5 kW/K. Some of the evaluated points were unable to get an UA-value, using a constant condensing temperature, and the LMTD method. This is due to, that the outgoing water from the condenser, is warmer than the condensing temperature (example of this is shown in Appendix B.1).



(a) Bitzer condenser (SWEP B25THx40).



(b) Sanden condenser (Alfa Laval CB24).

Figure 4.3: UA-value of the condensers used in the two heat pumps.

The condenser from Alfa Laval (Figure 4.3b) shows no trend of increase in UA-value as the compressor speed increases. It rather shows an opposite trend where UA-value decreases for a certain heating capacity with an increase of compressor speed. The data points within a certain compressor speed are however showing trends depending on evaporation and condensation temperature.

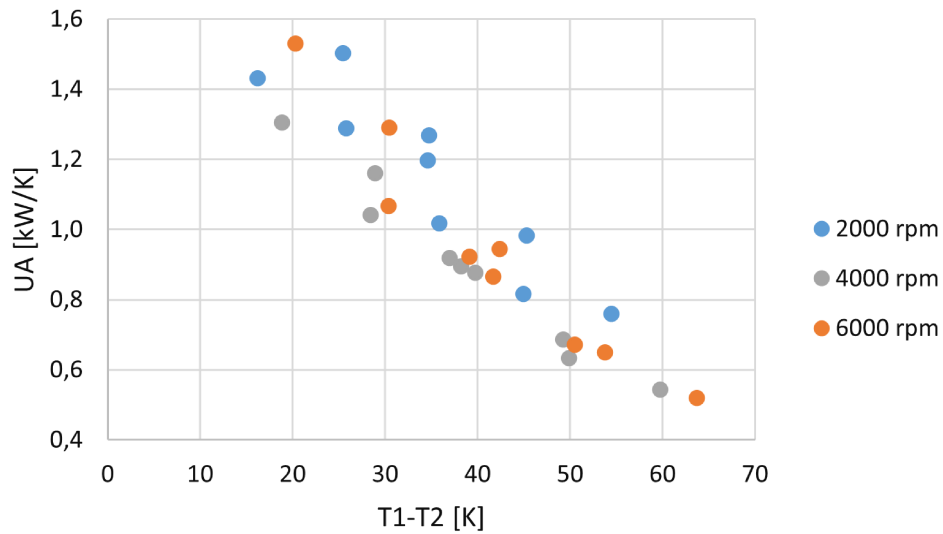
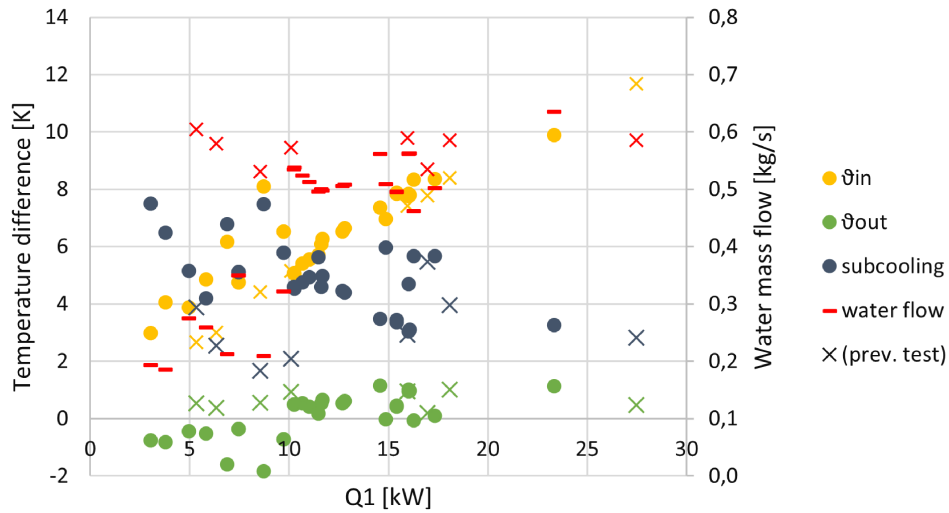


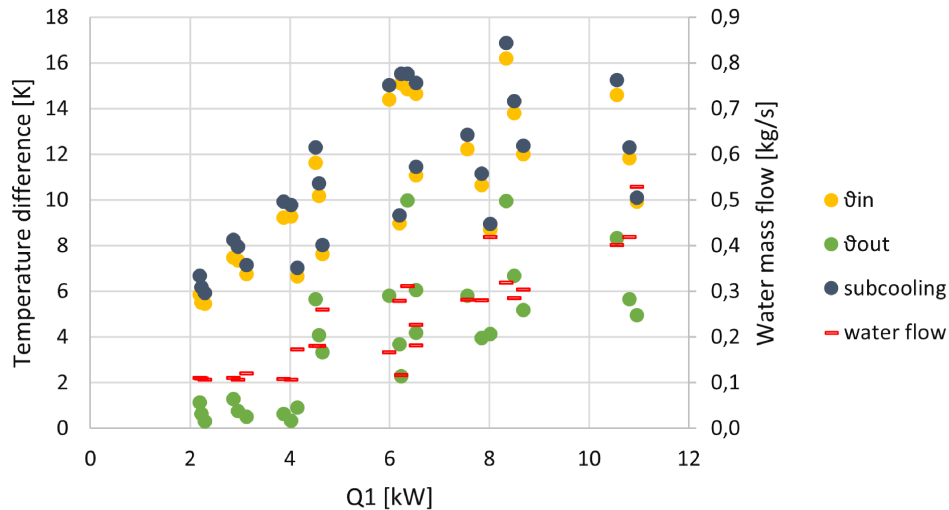
Figure 4.4: UA-value of the Sanden condenser with temperature lift.

This can be illustrated when looking at the UA-value as a function of the temperature lift (Figure 4.4). A clear trend of decrease in UA-value can be seen as the temperature lift is increased.

The UA-value determines the temperature differences between the water and the condensing refrigerant. An illustration of the temperature differences as a function of heating capacity is shown in Figure 4.5 together with the subcooling. Figure 4.5 also shows the variation of water mass flow, which in turn affect the temperature differences and hence the UA-value. This can be observed when comparing two points with approximately the same heating capacity but with different water flows.



(a) Bitzer condenser (SWEP B25THx40).



(b) Sanden condenser (Alfa Laval CB24).

Figure 4.5: Inlet/outlet temperature difference in condenser and subcooling.

The Bitzer condenser (Figure 4.5a) shows an increase of inlet temperature difference (ϑ_{in}) with higher heating capacity, while the outlet temperature difference (ϑ_{out}) is between -2 and +2 K. Figure 4.5a also illustrates points (below 0 K) where the outgoing water is warmer than the refrigerant condensation temperature. This comes as a result of water being heated by the vapor cooling process of the refrigerant leaving the compressor.

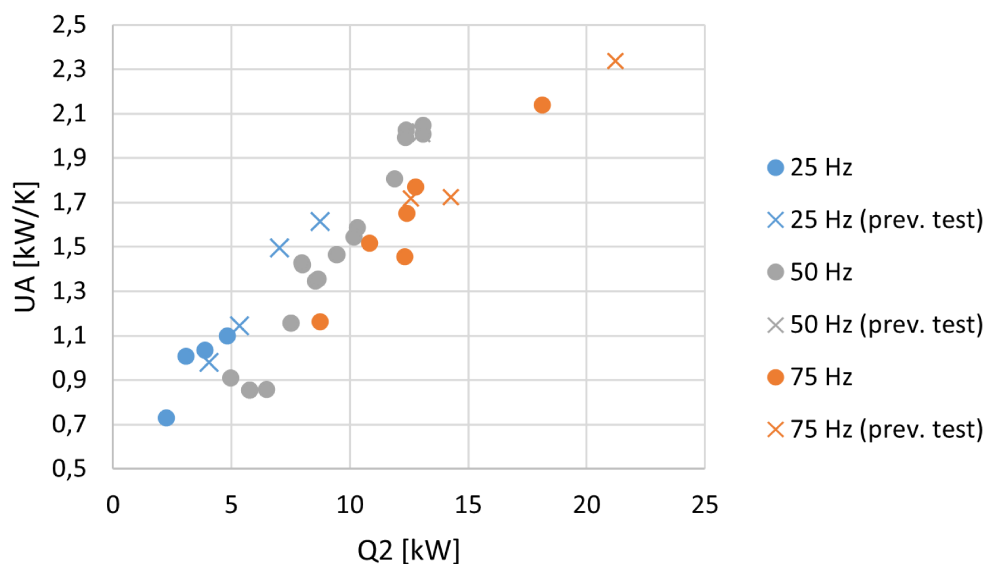
The Sanden condenser (Figure 4.5b) shows an increase of both temperature differences as the heating capacity increase. At low heating capacities between 2-4 kW, which corresponds to compressor speed 2000 rpm, the temperature

difference at the outlet (ϑ_{out}) is between 0-2 K. With an increase of compressor speed the outlet temperature difference reach up to 10 K. The subcooling in the condenser can also be observed to increase as the heating capacity increase.

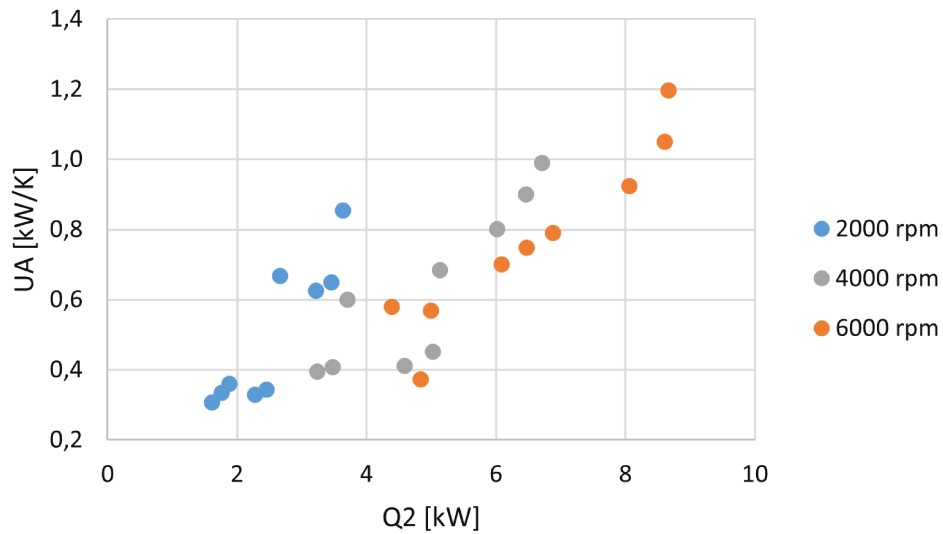
In the Sanden condenser (Figure 4.5b) it can be seen that the subcooling of the refrigerant shows to be higher than the temperature difference at the water inlet ϑ_{in} . This behavior can also be observed at the lower heating capacities in the Bitzer condenser (Figure 4.5a). This is an irregularity since it would indicate that the refrigerant is being subcooled below the water temperature.

4.3 Evaporator performance

The evaporator performance (UA-value) is shown as a function of the cooling capacity in Figure 4.6. The evaporator from SWEP (Figure 4.6a) used in the Bitzer heat pump shows an increase of the UA-value as the cooling capacity increases, the trend is the same for all speeds of the compressor. The UA-value also shows to be lower for the same amount of cooling capacity when increasing the compressor speed. Higher compressor speed while the cooling capacity is maintained is then related to a decrease of the evaporation temperature.



(a) Bitzer evaporator (SWEP F85Hx20/1P-NC-M).

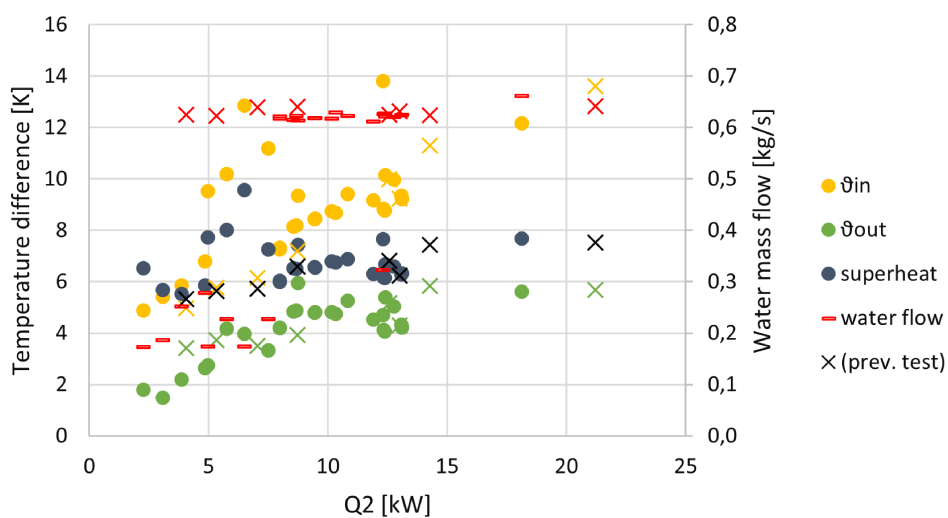


(b) Sanden evaporator (Alfa Laval CB24).

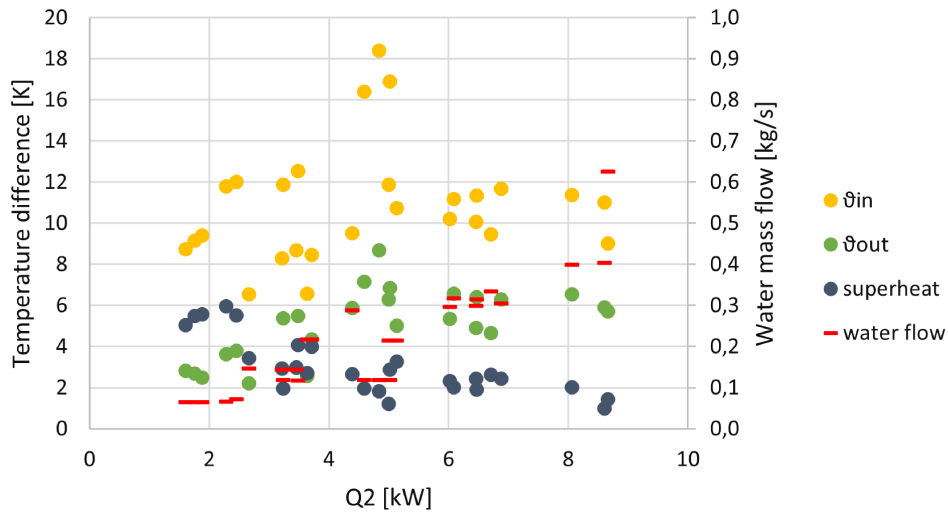
Figure 4.6: UA-value of the evaporators used in the two heat pumps

The Alfa Laval evaporator (Figure 4.6b) generally shows an increase of UA-value with higher cooling capacity for the different compressor speeds. Like the evaporator in the Bitzer heat pump, it also often has a higher UA-value for a lower compressor speed at the same cooling capacity.

In Figure 4.7 the temperature differences at the inlet and outlet are shown, along with the superheating and the variation of water mass flow in the evaporator.



(a) Bitzer evaporator (SWEP F85Hx20/1P-NC-M).



(b) Sanden evaporator (Alfa Laval CB24).

Figure 4.7: Inlet/outlet temperature difference in evaporator and superheating.

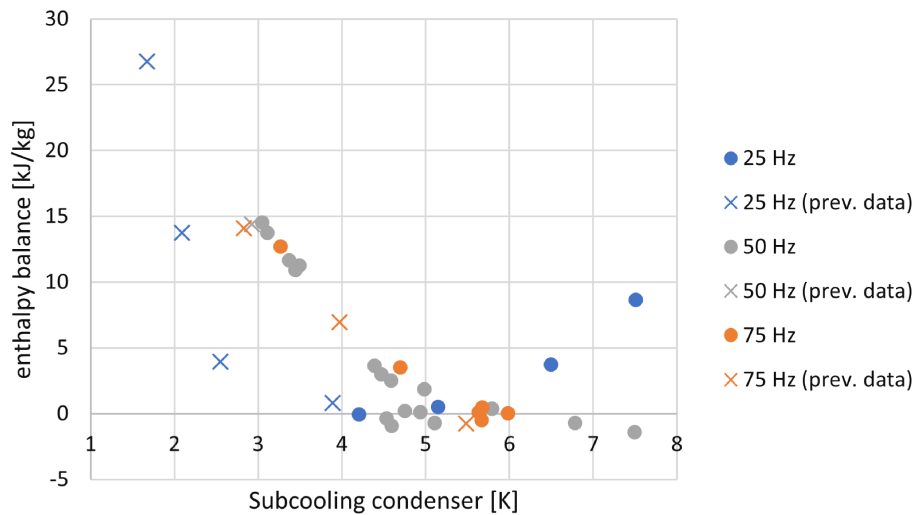
There is an increase in the temperature differences ϑ_{in} and ϑ_{out} with an increase of cooling capacity in the Bitzer evaporator (4.7a), while superheat in the evaporator is fairly constant at 6-8 K. At the lowest cooling capacities, the superheat can be observed as larger than the temperature difference ϑ_{in} . This is irregular and implies that the refrigerant is being superheated further than the temperature of the incoming water.

In the Sanden evaporator (Figure 4.7b) the temperature difference at the outlet (ϑ_{out}) shows an increase with higher cooling capacities, while the inlet (ϑ_{in}) temperature difference varies over the interval. The superheat can be observed to decrease with an increase of heating capacity in the Sanden evaporator.

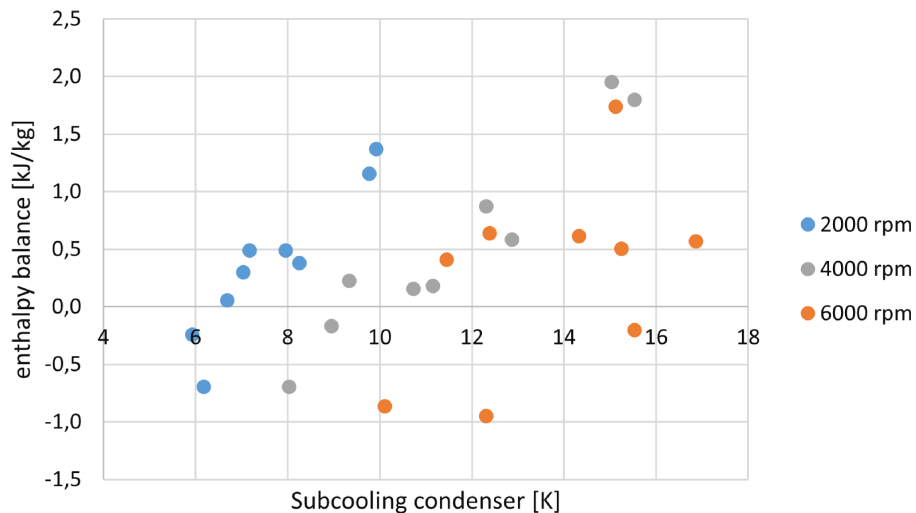
The water flow in the Sanden evaporator (Figure 4.7b) generally increased as the cooling capacity increased. Comparing the two points at cooling capacity of around 8.6 kW, it can be seen that the point with higher water flow shows a 2 K lower temperature difference ϑ_{in} , which results in a higher UA-value. The experimental point with higher water flow is related to a 10 K lower condensation temperature compared to the point with lower water flow, which means that refrigerant mass flow is lower. The difference in refrigerant mass flow between the two points however, is very small compared to the difference in water mass flow.

4.4 Internal heat exchanger

The enthalpy loss of the hot fluid from the condenser should be equal to the enthalpy gain of the gas from the evaporator, due to the overtime equal mass flow on both sides. The results (Figure 4.8) are based on the temperatures of the refrigerant at the in- and outlet on both sides, also known as sensible enthalpy change, which does not account for phase change occurring on either side in the internal heat exchanger. In Figure 4.8 the enthalpy difference between the two sides ($\Delta h_{suction} - \Delta h_{liquid}$) is shown, assuming pure liquid and pure gas entering, as a function of degrees subcooling of the refrigerant after the condenser.



(a) Bitzer Internal heat exchanger (SWEP B10THx30).



(b) Sanden internal heat exchanger (Pentaprop condenser).

Figure 4.8: Enthalpy balance of the internal heat exchanger.

The internal heat exchanger in the Bitzer heat pump (Figure 4.8a) shows the smallest difference in enthalpies when there is around 5 K of subcooling. When subcooling is below 5 K the sensible enthalpy change is larger on the suction side than on the liquid side.

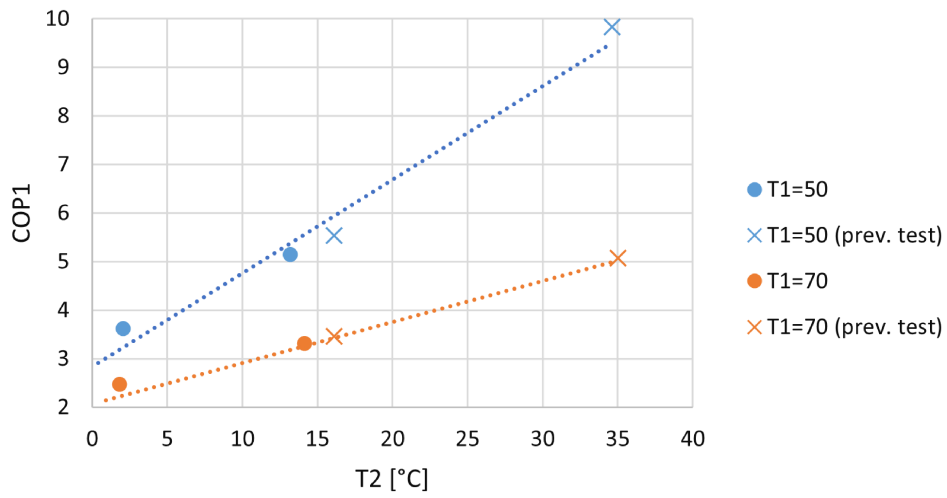
The amount of condenser subcooling in the Sanden heat pump is generally higher (4.8b) than the points measured in the Bitzer heat pump. The sensible enthalpy for the two sides is generally also more equal (closer to zero) and does not show any clear trend to depend on the amount of subcooling in the condenser.

4.5 Coefficient of performance

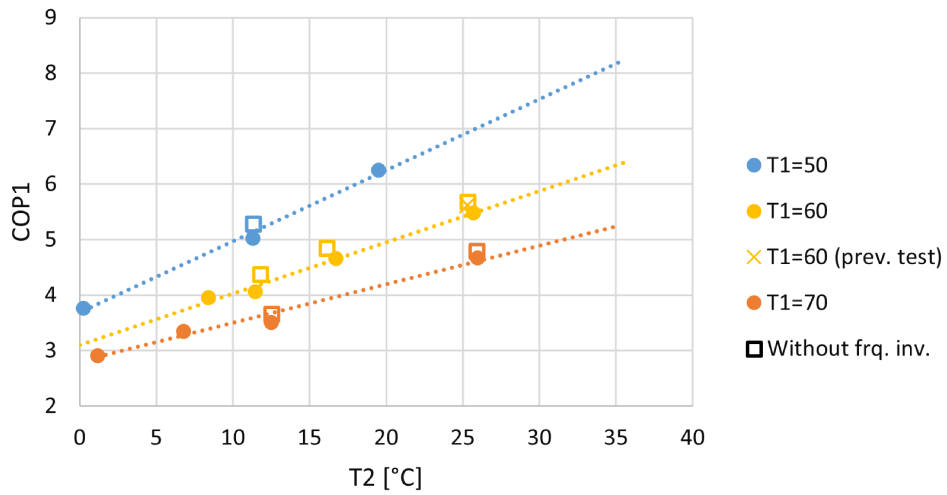
The COP for heating is shown in the following section. How it is varying with the different compressor speeds and also the temperature lift (T_1-T_2) is shown in Figures 4.9 - 4.10. Since evaporation temperatures differ a bit for the different condensation temperatures, compressor speeds and also between heat pumps, trend lines are plotted in the graphs for a better comparison. Data with the heating and cooling capacity as well as the compressor power can be found in Appendix E.

4.5.1 Bitzer heat pump

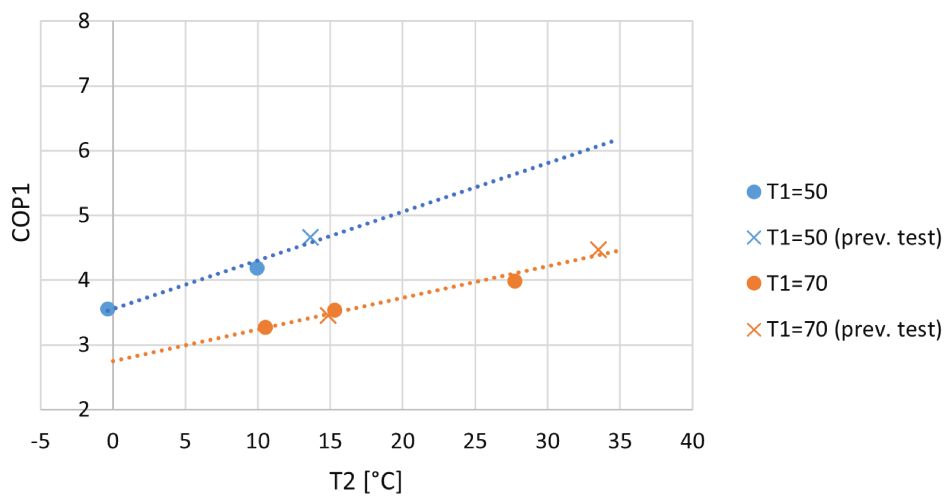
Generally, it can be seen in Figures 4.9a - 4.9c that for all compressor speeds the COP is increasing with a smaller temperature lift. A smaller temperature lift meaning a higher COP with increased evaporation temperature, and also further increase of COP by lowering the condensation temperature.



(a) Compressor speed 25 Hz.



(b) Compressor speed 50 Hz.



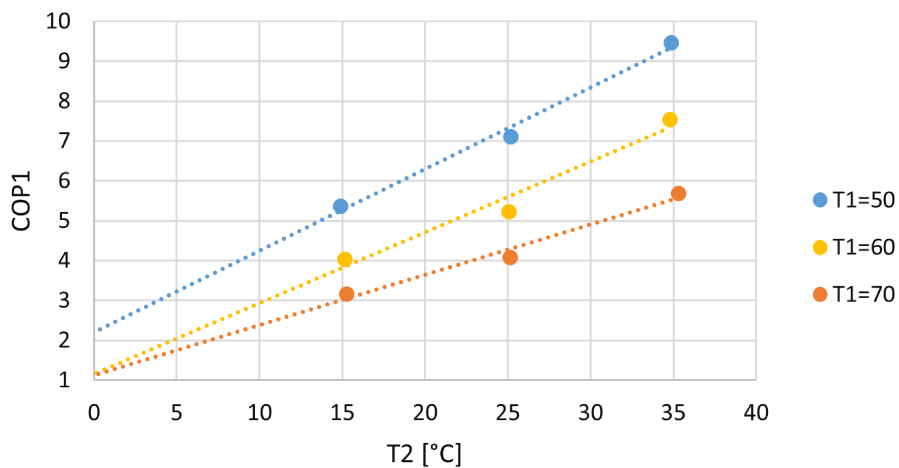
(c) Compressor speed 75 Hz.

Figure 4.9: COP of the Bitzer heat pump.

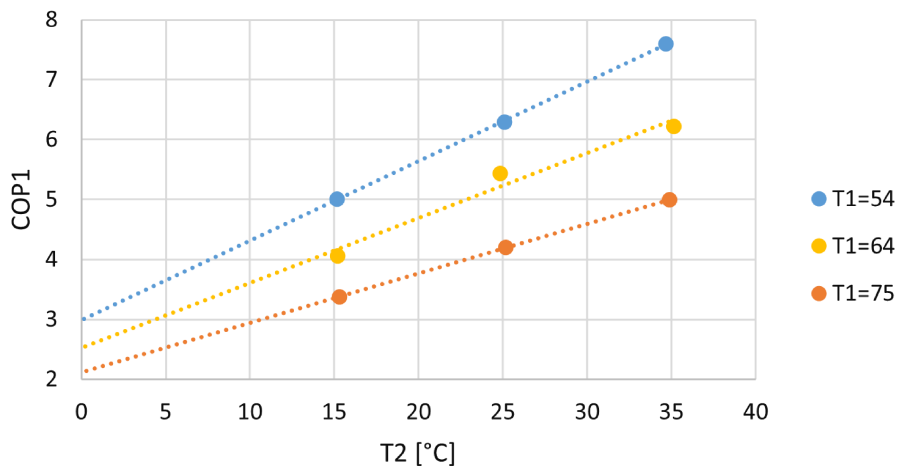
Running the Bitzer compressor at 50 Hz (Figure 4.9b) is shown to be most beneficial for almost all temperatures in terms of COP. An exception would be for a low temperature lift with a condensation temperature of 50 °C and with higher evaporation temperatures, where 25 Hz (Figure 4.9a) seems to be able to achieve a higher COP. For higher temperature lifts ($T_2 = 0$) a higher frequency than 25 Hz is required. Running compressor at 75 Hz (Figure 4.9c) does not show higher COP for any condensation or evaporation temperature compared to lower speeds.

4.5.2 Sanden heat pump

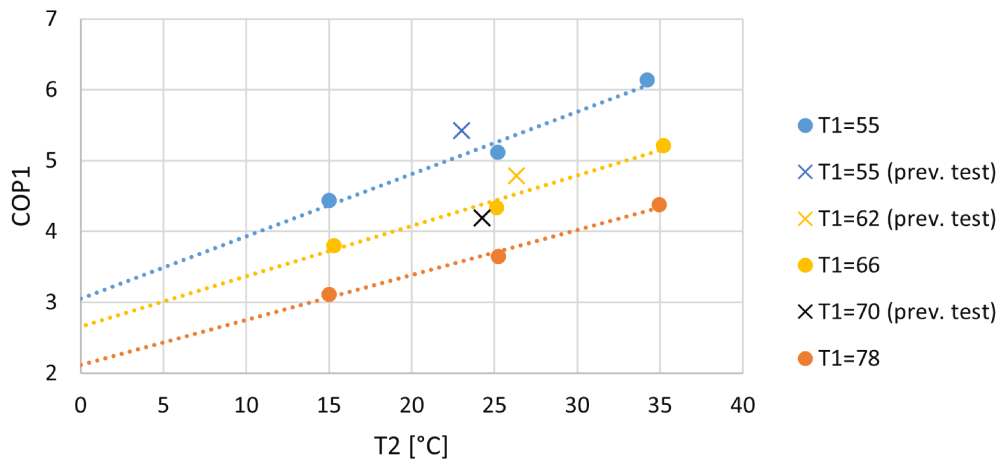
The tests made on the heat pump have approximately the same evaporation temperatures for all speeds. The condensation temperatures is however increasing a bit as the speed of the compressor increases.



(a) Compressor speed 2000 rpm.



(b) Compressor speed 4000 rpm.



(c) Compressor speed 6000 rpm.

Figure 4.10: COP of the Sanden heat pump.

As an overall trend for the different speeds, the COP increases with a smaller temperature lift. When the heat pump is running on high evaporation temperatures, the highest COP is achieved at 2000 rpm (Figure 4.10a). This is at least for condensation temperatures 50 and 60 °C, while 70 °C condensation could be either 2000 or 4000 rpm.

When temperature lift is increasing and evaporation temperatures are 25 °C a slightly higher COP is achieved with 4000 rpm (Figure 4.10b) for condensation temperatures 60 and 70 °C, while temperatures of around 50-54 °C seems more beneficial at 2000 rpm.

If the evaporation temperature is reduced to 15 °C, 2000 rpm shows the highest COP for low condensation temperature (50 °C). Keeping low evaporation temperature while increasing the condensation temperature above 60 °C proves best for the speed of 4000 rpm. Running the compressor at the highest speed of 6000 rpm (Figure 4.10c) shows no sign of being beneficial in terms of COP for any of the experimental points carried out within this research.

Further analysis of the results from this chapter, such as speculations addressing the optimality of the inconclusive results, are presented in the Discussion (Chapter 5).

Chapter 5

Discussion

The following chapter analyses the result of the experiments. Graphs are sometimes included to better support the discussion around the result. For some of the previous data of the Bitzer heat pump, the temperature difference between the water inlet and outlet (above 3 K) for the condenser and evaporator, was not fulfilled. This was for the Bitzer compressor at a speed 25 Hz and should be taken into consideration when analyzing the results.

5.1 Compressor

The Bitzer compressor (Figure 4.1a) running at 50 Hz showed the highest isentropic efficiency throughout the span of pressure ratios made in the experiment. The differences between running the compressor on 50 Hz compared to 25 or 75 Hz are frequently above 5 %. This can be due to several types of losses in the compressor. For low speeds, leakage losses through valves can have a larger impact on efficiency. At higher speeds, the pressure drop through valves will increase. Other factors such as mechanical losses, heating of the gas and the efficiency of the electric motor also have an effect on isentropic efficiency. Further evaluation would be needed to conclude on the reasons for the differences in efficiency between the different speeds.

The Sanden compressor (Figure 4.1b) results showed an overall lower isentropic efficiency than the Bitzer compressor. However, it also showed a lower efficiency compared to the previous tests for 6000 rpm. This is one indication that the compressor is not running optimally at this speed. A possibility is that there is a lack of oil in the heat pump. The oil is mixed with the refrigerant in the system so an overcharge of refrigerant means that there is not a sufficient amount of oil located in the compressor at any given time. The internal volume in the heat pump has increased (since evaluated in [7]) with the new internal heat exchanger which means more internal area for the oil to gather in. That will result in a low volumetric efficiency which could also be seen in Figure 4.2b, especially at 6000

rpm. A further evaluation of this would be of interest. Adjusting the refrigerant charge to meet the criteria of sufficient subcooling at the lowest speed of the compressor is thought to be the reason for this. This means that there is an overcharge of the refrigerant at 6000 rpm. Analyzing one of the experimental points and comparing it with a previous test, the refrigerant overcharge and hence lack of oil, seems to cause 5 % lower mass flow through the compressor and at the same time 5 % higher compressor work. The evaporation temperature differs with around 3 K between the compared points (which affect the ideal compressor work). These factors cause the isentropic efficiency to be 9 % lower than the corresponding previous test. The two tests were made at compressor speed 6000 rpm and had the same (within 1 K) condensation temperature and superheat before the compressor.

The volumetric efficiency was in most cases decreasing with an increased pressure ratio, which is the expected outcome. The decrease of efficiency with increasing pressure ratio was found to be greater for the Bitzer compressor. This is thought to be due to the dead space which results in the re-expansion of compressed gas occurring in reciprocating compressors. While the scroll compressor from Sanden lacks dead space, the decrease of efficiency could instead be because scroll compressors have a fixed built-in compression ratio. This would then lead the compressor to have either higher or lower pressure in the compressor chamber at exhaust compared to the discharge line.

At the lower pressure ratios (below 3) in the Bitzer compressor, the difference in efficiency occurring at a certain pressure ratio and compressor speed, can however not be explained by the re-expansion phenomena, since this should have a larger influence with increasing pressure ratio.

The Sanden compressor instead showed a steady decrease of volumetric efficiency for 2000 and 4000 rpm. Speed 6000 rpm on the other hand showed a constant volumetric efficiency throughout the pressure ratio domain, which is of course highly unsuspected. With a scroll compressor it is expected that the decay of efficiency is smaller than the reciprocating one when increasing the pressure ratio. However, being constant at around 80 % while also being lower than the Bitzer compressor is unexpected. Furthermore, a comparison from the previous study [7] on the compressor also shows that 6000 rpm has considerably lower volumetric efficiency than those experiments. Not only, but 4000 rpm also showed lower efficiency than what was found in that study, which furthermore showed higher volumetric efficiency for 4000 and 6000 compared

to 2000 rpm. The explanation for this would then be the amount of oil traveling with the refrigerant as explained previously in this section. The low amount of oil will then cause insufficient sealing between the orbiting scroll and the fixed scroll, which then disturbs the compression. Since volumetric efficiency otherwise is expected to increase with a smaller pressure ratio or (temperature lift), and now being constant means that the largest difference in volumetric efficiency would be at the lowest pressure ratio.

5.2 Condenser performance

The condenser from SWEF (Figure 4.3a) showed different results for the various compressor speeds. 50 Hz did not have any relation between UA-value and heating capacity, nor did it have any relation with the temperature lift. 75 Hz showed two different trends that increased with heating capacity. However a relation between the trends could not be found, either with condensation/evaporation temperature or temperature lift. The temperature differences in the condenser did however prove it to be functioning well. The outlet ϑ_{in} temperature difference was kept small for the whole range, which means that the outlet temperature of the water and the refrigerant condensation temperature correspond very well.

The Alfa Laval condenser (Figure 4.3b) had similar UA-values for all the speeds of the compressor. The variation within the speeds could instead be seen with a change in the temperature lift. For a certain speed of the compressor, an increase in the temperature lift means a decrease in the mass flow of the refrigerant. The mass flow of the refrigerant being (with at least 1/7 of the water flow) the lower of the two media flows in the heat exchanger, could have an influence on the heat transfer coefficient (U) in the condenser. Hence a lower refrigerant mass flow would lead to a decrease in the heat transfer coefficient. Another explanation is that with an increase of pressure ratio, the temperature difference between refrigerant at compressor outlet and the condensation temperature increases. This means that a larger area of the condenser is used for cooling the vapor from the compressor and leaves less area for condensation, which decreases the UA-value.

A UA-value that is constant or decreases with an increase of compressor speed means that the LMTD between the two mediums in the heat exchanger has increased instead. This in turn is a result of an increase in the temperature

difference ϑ_{in} (incoming water and refrigerant) and/or ϑ_{out} (outgoing water and refrigerant). Temperature difference ϑ_{in} is determining the amount of subcooling in the condenser, which was increasing as the compressor speed went up (further detail in Appendix D). With increasing subcooling, the heat transfer area for condensation instead decreases, which lowers the UA-value. Ideally, the temperature difference ϑ_{out} should be kept to a minimum (or even negative if utilizing desuperheat region). For the experiments at 2000 rpm the temperature difference ϑ_{out} was between 0-1 K. With an increase of both compressor speed and condenser subcooling it reached up to 10 K for 6000 rpm. For a given water outlet temperature in the condenser, the effects of the big temperature difference ϑ_{out} could be reduced by decreasing the mass flow of the water (details can be seen in Appendix C).

The Sanden condenser (Figure 4.5b) constantly showed a larger subcooling than the temperature difference ϑ_{in} , something that also occurred for low heating capacities in the Bitzer condenser (Figure 4.5a). In the Sanden experiments, this would seem to be a systematic error and might be a sign of temperatures not being measured correctly. This is despite the fact that capillary tubes were welded inside the pipes of both the water and refrigerant circuit.

5.3 Evaporator performance

Evaporator from SWEP showed an increasing trend for the UA-value with higher cooling capacity, for all compressor speeds. The UA-values are generally lower than the ones for the condenser in the same heat pump, which is partially due to a smaller area of heat exchange.

Alfa Laval evaporator also showed an increase of UA-value as the cooling capacity was increased. However, the temperature differences at the inlet and outlet were in this case considerably larger than the Bitzer evaporator. This is despite the fact that the amount of superheating was lower in the Sanden experiments compared to the Bitzer experiments. In other words, the temperature difference at the inlet ϑ_{in} is many times considerably higher than the superheating (example of the temperature profile in Appendix B.2). This means that evaporation temperatures have to be much lower than the corresponding heat source, which in turn means that the Sanden compressor needs to make higher-temperature lifts even if the heat source is at the same temperature for the two heat pumps.

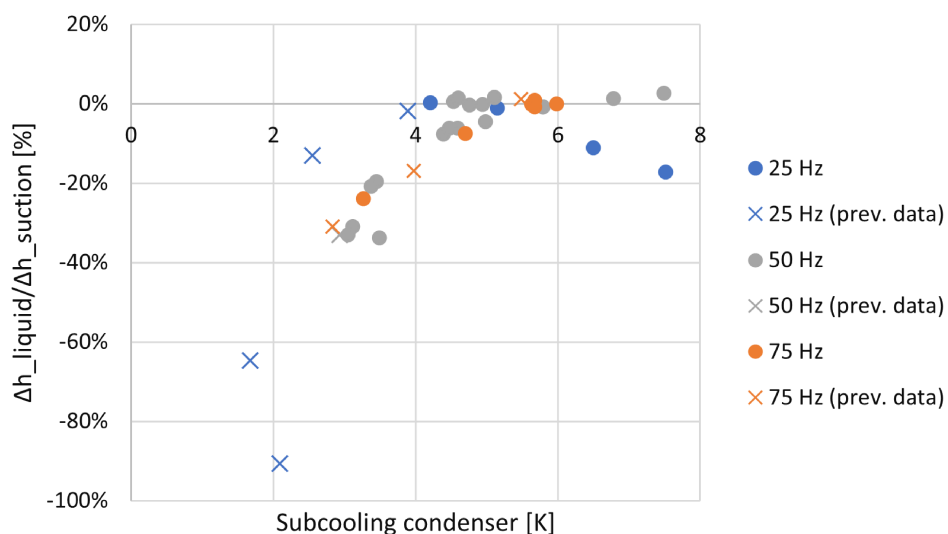
The results showed that the UA-value was decreased for the same cooling capa-

city when increasing the compressor speed, this trend was for both heat pumps. The amount of superheat in the evaporator has an effect on the UA-value. However, in the Bitzer heat pump the superheat was fairly constant in all of the experiments and in the Sanden heat pump the superheat was decreasing as the compressor speed increased. The superheat is hence not likely to be the reason for the difference in the UA-values.

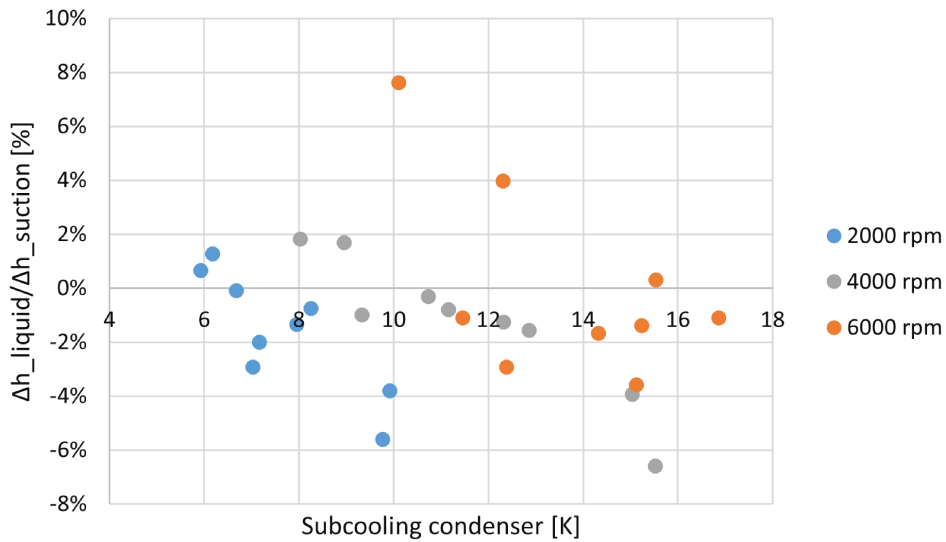
5.4 Internal heat exchanger

The SWEP internal heat exchanger used in the Bitzer heat pump showed results where most of the experimental points were on the positive side of the enthalpy balance. This indicates that the sensible enthalpy change is larger on the suction side. This in turn would indicate that more latent enthalpy change (phase change) is occurring on the liquid side of the internal heat exchanger. Figure 4.8a also shows an increasing difference between the two sides when subcooling decreases below 5 °C, why suspicion of some fraction of the refrigerant being condensed in the internal heat exchanger.

The Sanden heat exchanger result also showed a majority of the measured points with higher sensible enthalpy on the suction side. Subcooling was generally higher with the lowest value of 6 K and there was no trend of a change in the difference as the subcooling increased. The difference between the suction and liquid side of the internal heat exchanger can be further evaluated as the difference in percent in Figure 5.1.



(a) Bitzer Internal heat exchanger (SWEP B10THx30))



(b) Sanden internal heat exchanger (Pentaprop condenser)

Figure 5.1: Enthalpy balance of the internal heat exchanger [%]

The results showed considerably lower difference percentage-wise in the internal heat exchanger for the Sanden heat pump (Figure 5.1b), with the highest difference being around 8 % enthalpy difference between suction and liquid side.

For the Bitzer heat pump internal heat exchanger the difference in percent is higher (Figure 5.1a). When subcooling was between 2-4 °C the results showed up to 34 % lower enthalpy on the liquid side compared to suction. Two previous tests made with subcooling between 0-2 °C showed an even larger difference of up to 90 %. When subcooling is increased to above 4 °C the difference is generally below 10 % except for one outlier at around 20 % even when subcooling is above 7 °C. This is indicating that there is not a homogeneous subcooling of the liquid.

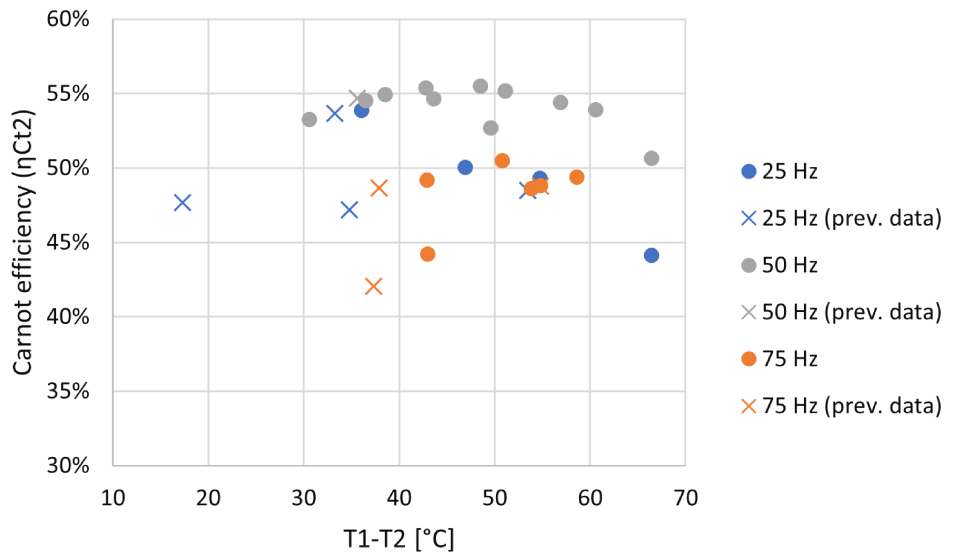
It can be seen that both heat pumps require a substantial amount of subcooling for a partial condensation not to occur in the internal heat exchanger. With the pressure measured at the inlet of the condenser, a pressure drop in the condenser will lead to the actual condensing pressure being lower than the measured one. This will make the actual subcooling smaller than the one measured in these experiments. For the Sanden condenser, this is something that could also be suspected when the required subcooling was between 4-6 K before vapor bubbles cleared from the sight glass.

5.5 Coefficient of performance

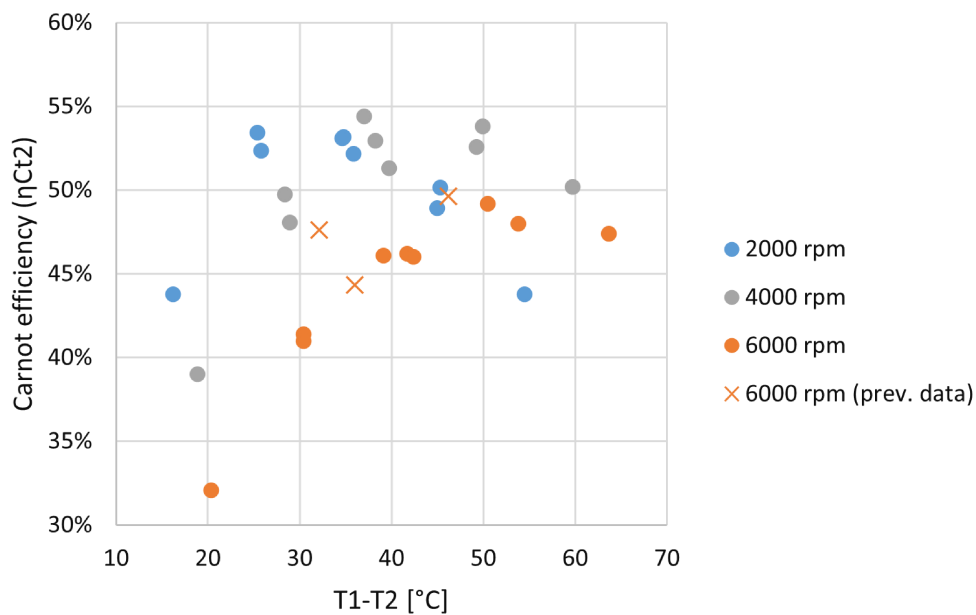
The Bitzer results showed that compressor speed 50 Hz overall gave the best COP. The heat pump was filled with a certain amount of refrigerant prior to the start of this thesis and was evaluated with this amount of charge. Since both isentropic and volumetric efficiency was found to be lower for the speeds 25 and 75 Hz, a suspicion could be that the charge would be more optimal for 50 Hz. However, when looking for signs of under- or overcharge in the system in terms of the amount of subcooling in the condenser and also superheat in the evaporator, no conclusions can be drawn. The amount of superheating and subcooling does not show any clear relationship with the speed of the compressor (see Appendix D for details). Other reasons could be those mentioned in the compressor efficiency (Section 5.1) for 25 and 75 Hz, where the effects on the efficiency of the compressor will also affect the COP. 25 Hz did show a result of higher COP at low condensation temperature together with a high evaporation temperature. This result is however based on a single measurement from a previous test, which should be taken into consideration.

From the Sanden results (4.10) it could be seen that the condensation temperature was increasing as the compressor speed increased. Results showed that 2000 rpm gave the highest COP for the lower temperature lifts. This is the speed when the heat pump is considered to be working under the right amount of charge. For higher temperature lifts, 4000 rpm resulted in a higher COP, at these temperature lifts (or pressure ratios) is also where the compressor showed a better volumetric and isentropic efficiency, which affects the COP. At the highest speed 6000 rpm it could be seen in comparison to the previous result that the COP, in this case, was lower. This is also the speed when the compressor did not seem to be working ideally and suffered from a lack of oil.

Another indication of the COP can be made when comparing with the Carnot efficiency for refrigeration, which is presented in Figure 5.2 as a function of the temperature lift.



(a) Bitzer heat pump



(b) Sanden heat pump

Figure 5.2: Carnot efficiency for refrigeration.

From Figure 5.2a it can be seen that the highest Carnot efficiency is around 55 % when the Bitzer compressor is running at 50 Hz. For 25 and 75 Hz, the Carnot efficiency is generally around 45-50 %. These values are considered to be within the acceptable range from literature.

The Carnot efficiency of the Sanden heat pump (Figure 5.2b) generally shows values between 45-55 % with some exceptions in the lower temperature lifts.

For these temperature lifts (around 20 °C) the Carnot efficiency is decreasing more with a higher speed of the compressor. This would then be the effect of having poor compression (due to lack of oil) which will affect the volume flow more significantly for lower temperature lifts.

5.6 Future Work

The primary future work would be for the heat pump with Sanden compressor since the plan is to implement it as an economizer. A more well-adopted internal heat exchanger should be incorporated in the heat pump, which will reduce the refrigerant charge of the system. For further evaluations of the heat pump with the current internal heat exchanger, the problem with the amount of charge for compressor speeds 4000 and 6000 rpm should be evaluated, investigate the possibility of a liquid receiver after the condenser. Secondly, a sufficient amount of oil in relation to the charge must also be evaluated. Finally, appropriate water flows through the heat exchanger should be evaluated to minimize the temperature differences between the water and refrigerant but also to decrease condensation temperature. This also regards decreasing the temperature difference between the heat source and evaporation temperature.

For further evaluation of the heat pump using the Bitzer compressor, assurance of sufficient subcooling in the condenser should be made in order to not have unnecessary condensation in the internal heat exchanger.

Chapter 6

Conclusion

Important facts that need to be considered for the conclusive statements are presented first. The condensation temperatures differ slightly from each other, more so as the compressor speed increases. The evaluated evaporation temperatures are not the same between the two but can be compared if assumed linear with evaporation temperature. Finally, there were indications that the Sanden heat pump suffered from overcharge at speeds 4000 and 6000 rpm. All these facts must be taken into consideration when comparing the two heat pumps.

The Bitzer compressor showed higher isentropic efficiency but lower volumetric efficiency when compared to the Sanden compressor on a per speed interval basis. An exception to this conclusion was found at the highest speed of the Sanden compressor, where its volumetric efficiency was lower than the Bitzer compressor. The evaporators of the two heat pumps showed an increase of UA-value as the cooling capacity increased, Bitzer heat pump had slightly higher UA-values in the same range of cooling capacity. There were, however, large differences between the inlet and outlet temperatures of the water compared to the refrigerant, in both heat pumps. The condenser in the Bitzer heat pump showed satisfactory UA-values which resulted in a low-temperature difference between refrigerant and water outlet. The UA-values of the condenser in the Sanden heat pump did not increase with compressor speed which then gave a large temperature difference between refrigerant and heat sink water, for the two higher compressor speeds. The internal heat exchanger in the Bitzer heat pump showed that there was a different sensible enthalpy between the two sides when the condenser subcooling was insufficient, especially for subcooling below 5K, indicating partial condensation in the internal heat exchanger instead. The Sanden heat pump had a higher subcooling (above 6 K) which also showed a better sensible enthalpy balance in the internal heat exchanger.

Lastly, conclusions regarding the COP at different speeds are presented. The comparison of the COP revealed that the highest value was achieved at the

lowest speed and for a small temperature lift. At the lowest speed, the Bitzer heat pump had a slightly higher COP for low condensation for all evaporation temperatures. Moreover, at high condensation temperature, the Sanden heat pump had a slightly higher COP at high evaporation temperature while the Bitzer heat pump showed to be better at low evaporation temperature. In the mid-range speed, 50 Hz and 4000 rpm, the Bitzer heat pump proved to have equal or better COP for the whole range of temperatures. The same result could be found for the highest speed 75 Hz and 6000 rpm where the Bitzer heat pump was equal to or slightly better than the Sanden heat pump.

Bibliography

- [1] E. Granryd *et al.*, *Refrigerating engineering*. Royal Institute of Technology, KTH, Department of Energy Technology, Division of Applied Thermodynamics and Refrigeration, 2009.
- [2] SWEP, “Refrigeration handbook.” Accessed 28 Sep 2021 URL: <https://www.swep.se/refrigerant-handbook/3.-compressors/3.2-compressor-types/>.
- [3] W. Kim and J. E. Braun, “Evaluation of the impacts of refrigerant charge on air conditioner and heat pump performance,” *International Journal of Refrigeration*, vol. 35, no. 7, pp. 1805–1814, 2012. URL: <https://www.sciencedirect.com/science/article/pii/S0140700712001533>.
- [4] I. Grace, D. Datta, and S. Tassou, “Comparison of hermetic scroll and reciprocating compressors operating under varying refrigerant charge and load,” *Purdue e-Pubs*, 05 2002. URL: https://www.researchgate.net/publication/228835812_Comparison_Of_Hermetic_Scroll_And_Reciprocating_Compressors_Operating_Under_Varying_Refrigerant_Charge_And_Load.
- [5] “Regulation (eu) no 517/2014 of the european parliament and of the council of 16 april 2014 on fluorinated greenhouse gases and repealing regulation (ec) no 842/2006 text with eea relevance,” Apr 2014. Accessed 28 Sep 2021 URL: <http://data.europa.eu/eli/reg/2014/517/oj>.
- [6] Danfoss, “Practical application of refrigerant r600a isobutane in domestic refrigerator systems,” 2000. Accessed 28 Sep 2021 URL: [http://folk.ntnu.no/skoge/book-cep/diagrams/additional_diagrams/more_on_refrigerants/isobutane\(R600A\)-Danfos.pdf](http://folk.ntnu.no/skoge/book-cep/diagrams/additional_diagrams/more_on_refrigerants/isobutane(R600A)-Danfos.pdf).
- [7] E. Forsgren, “Evaluation of an economizer solution for a heat pump,” Master’s thesis, Royal Institute of Technology KTH, 2020. URL: <http://www.diva-portal.org/smash/get/diva2:1470364/FULLTEXT01.pdf>.
- [8] M. El-Morsi, “Energy and exergy analysis of lpg (liquefied petroleum gas) as a drop in replacement for r134a in domestic refrigerators,” *Energy*, vol. 86,

pp. 344–353, 2015. URL: <https://www.sciencedirect.com/science/article/pii/S0360544215004892>.

- [9] “Reciprocating compressors ecoline.” "Image of Bitzer compressor". Digital image of Bitzer compressor overview. Accessed 28 Sep 2021. URL: https://www.bitzer.de/shared_media/documentation/kp-100-1-en.pdf.
- [10] "Image of Sanden compressor". Digital image of Sanden compressor overview. Accessed 28 Sep 2021. URL: <https://sanden.wpengine.com/wp-content/uploads/2019/02/SHS33-Fact-Sheet-SIEUK180035A.pdf>.

Appendix A

Components, equipment & measurement points



Figure A.1: Bitzer heat pump

Number	Type	Manufacturer/Model
1	Compressor	Bitzer 4EESP-4Z-40S
2	Internal heat exchanger	Kylma B10THx30/1P-SC-M.
3	Evaporator	Kylma F85Hx20/1P-NC-M
4	Condenser	Kylma B25THx40
5	Expansion valve	Carel EVD evolution
6	Pressure transducer p_A	Carel SPKT0021CO
6	Temperature T_A	Thermocouple T-type
7	Pressure transducer p_B	Yokogawa EJA510E
7	Temperature T_B	Thermocouple T-type
8	Pressure transducer p_C	Yokogawa EJA510E
8	Temperature T_C	Thermocouple T-type
9	Temperature T_D	Thermocouple T-type
10	Temperature T_F	Thermocouple T-type
11	Temperature T_G	Thermocouple T-type

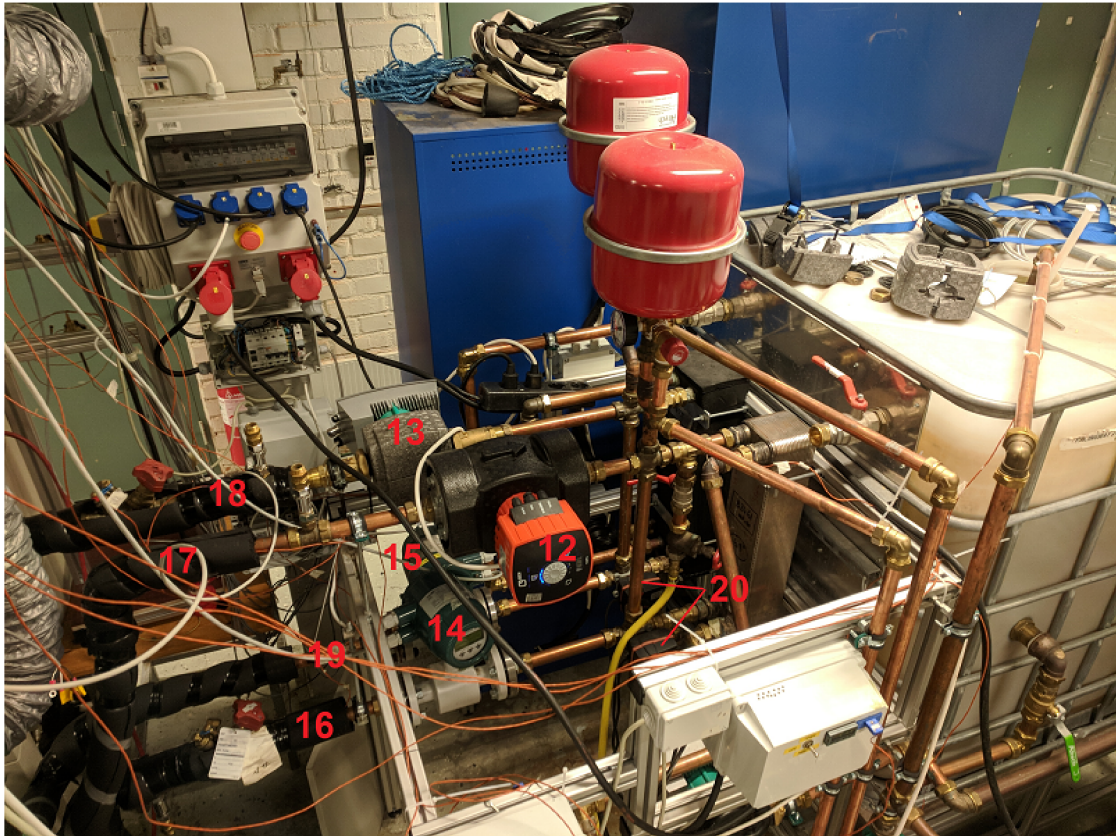


Figure A.2: Measurement points on water circuit

Number	Type	Manufacturer/Model
12	Water pump heat sink	Calio 32-120
13	Water pump heat source	Wilo stratos 30/1-12
14	Water flow measure (\dot{V}_{12} / heat sink)	Yokogawa RXF025G
15	Water flow measure (\dot{V}_{21} / heat source)	Yokogawa AXF025G
16	Temperature T_{11}	Thermocouple T-type
17	Temperature T_{12}	Thermocouple T-type
18	Temperature T_{21}	Thermocouple T-type
19	Temperature T_{22}	Thermocouple T-type
20	Three way valves	Esbe 12500100 62p

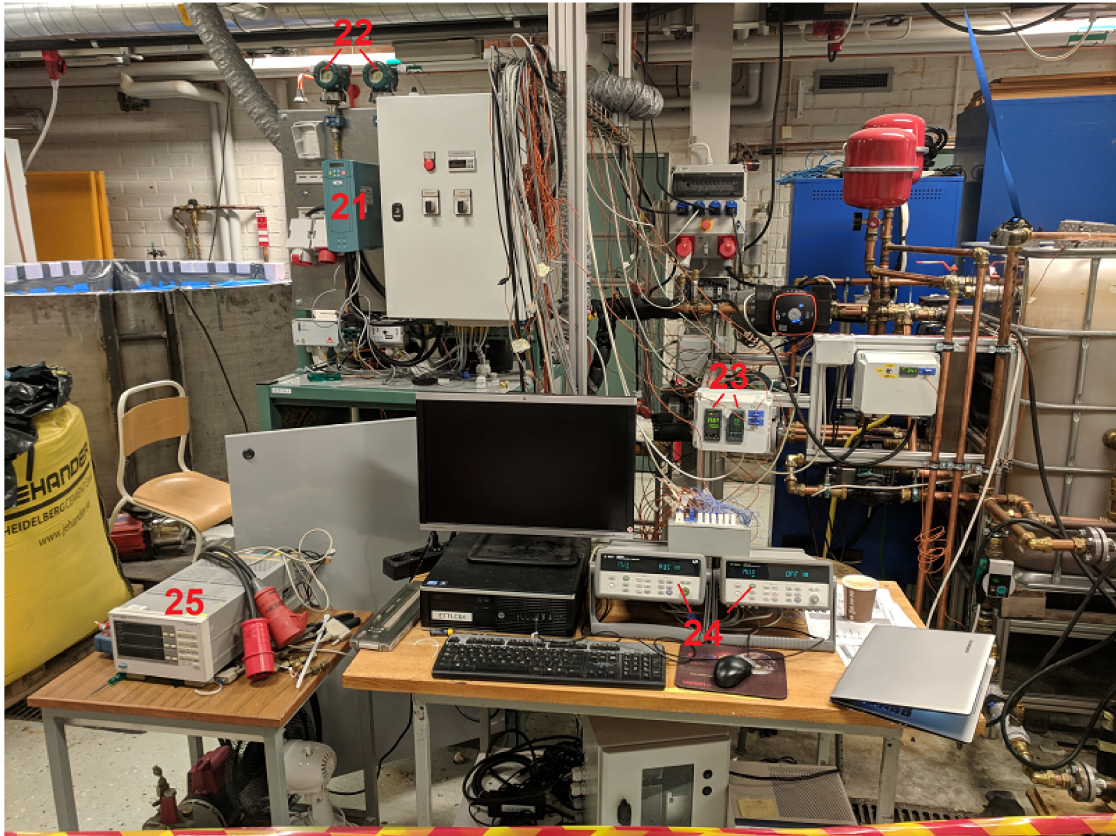


Figure A.3: Measurement equipment

Number	Type	Manufacturer/Model
21	Frequency inverter	Eurotherm 650 series
22	Absolute Pressure Transmitter	Yokogawa EJA510E
23	PID regulators	Eurotherm 2408/3508
24	Data acquisition units	Agilent 34972A/34970A
25	Digital power meter	Yokogawa WT130

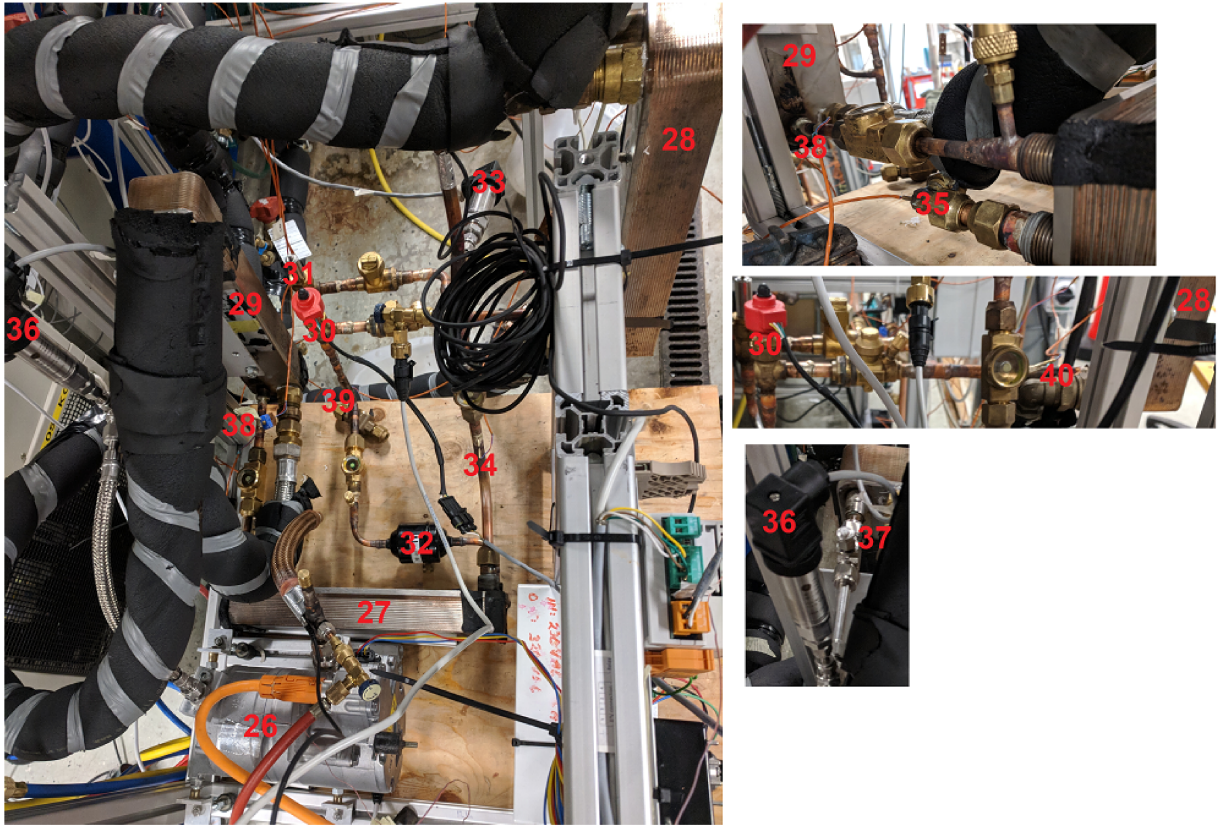


Figure A.4: Sanden heat pump

Number	Type	Manufacturer/Model
26	Compressor	Sanden SH33
27	Internal heat exchanger	Pentaprop condenser 31 plates
28	Evaporator	Alfa Laval CB24
29	Condenser	Alfa Laval CB24
30	Expansion valve large	Carel EVD evolution
31	Expansion valve small	Carel EVD evolution
32	Filter drier	
33	Pressure transducer p_A	Druck Unik 5000
34	Temperature T_A	Thermocouple T-type
35	Temperature T_B	Thermocouple T-type
36	Pressure transducer p_C	Druck Unik 5000
37	Temperature T_C	Thermocouple T-type
38	Temperature T_D	Thermocouple T-type
39	Temperature T_F	Thermocouple T-type
40	Temperature T_G	Thermocouple T-type

Appendix B

Temperatures in HEX

B.1 Bitzer

Figure B.1 demonstrates one case when the LMTD method does not work due to higher temperature of the outlet water than the condensation temperature. Figure B.1 also illustrates an irregularity where the heat sink inlet temperature appears to be higher than the refrigerant outlet temperature.

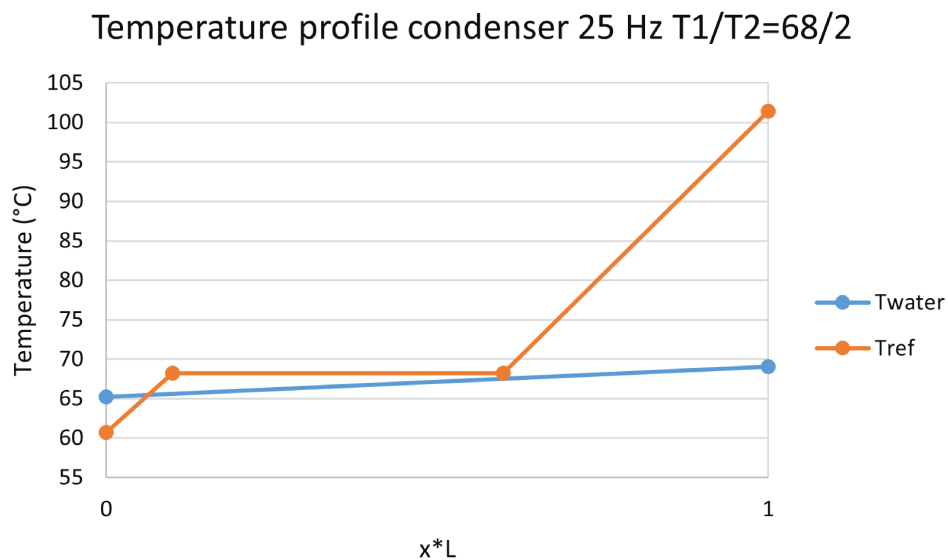


Figure B.1: Temperature profile in the condenser (length x only estimated and not calculated)

Figure B.2, showing the temperature profile in the evaporator in one experiment, which illustrates an irregularity where the outlet of the refrigerant appears to reach a higher temperature than the heat source inlet temperature.

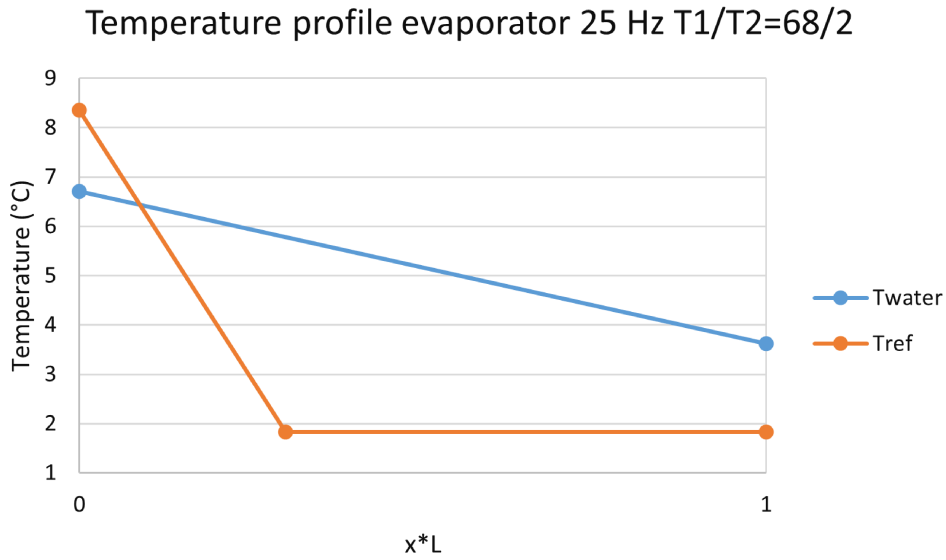


Figure B.2: Temperature profile in the evaporator (length x only estimated)

The temperature differences ϑ_{in} and ϑ_{out} in the condenser (Figure B.3) and evaporator (Figure B.4) for all experiments.

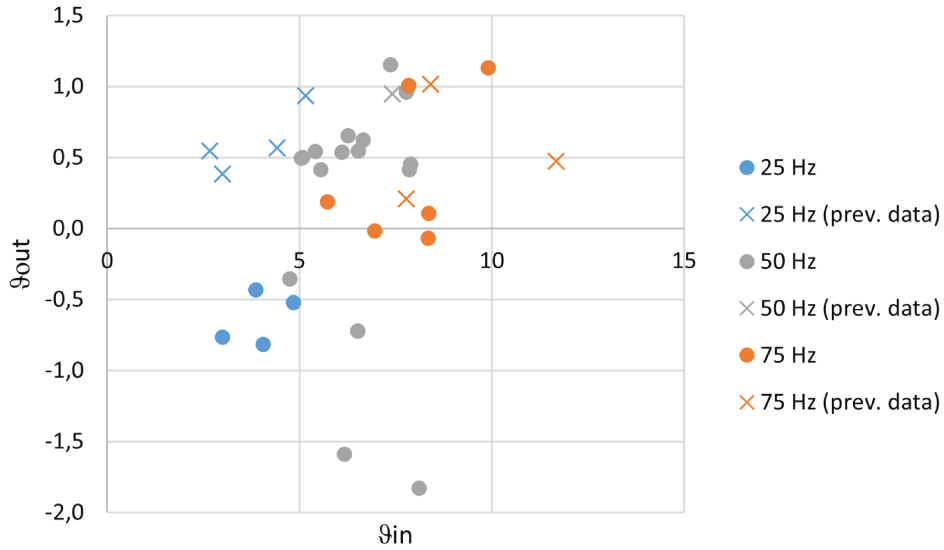


Figure B.3: Temperature differences in condenser (negative values not valid for LMTD).

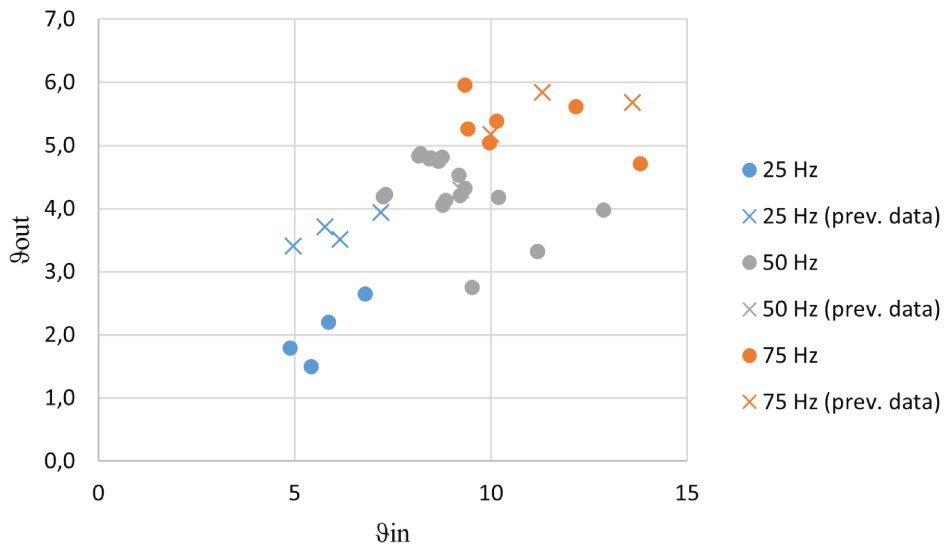


Figure B.4: Temperature differences in evaporator.

Figures B.5-B.6 showing the temperature profile of the internal heat exchanger in the Bitzer heat pump. Figure B.5 illustrates when the sensible enthalpy change of the refrigerant in the liquid and suction line are the same, and Figure B.6 when they are different.

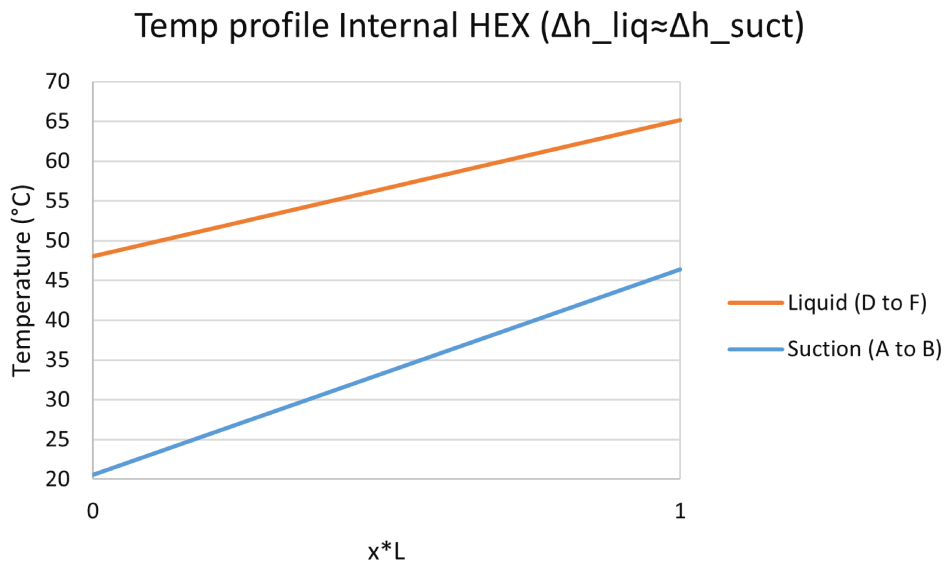


Figure B.5: Example of temperatures when the sensible enthalpy is equal for liquid/suction side.

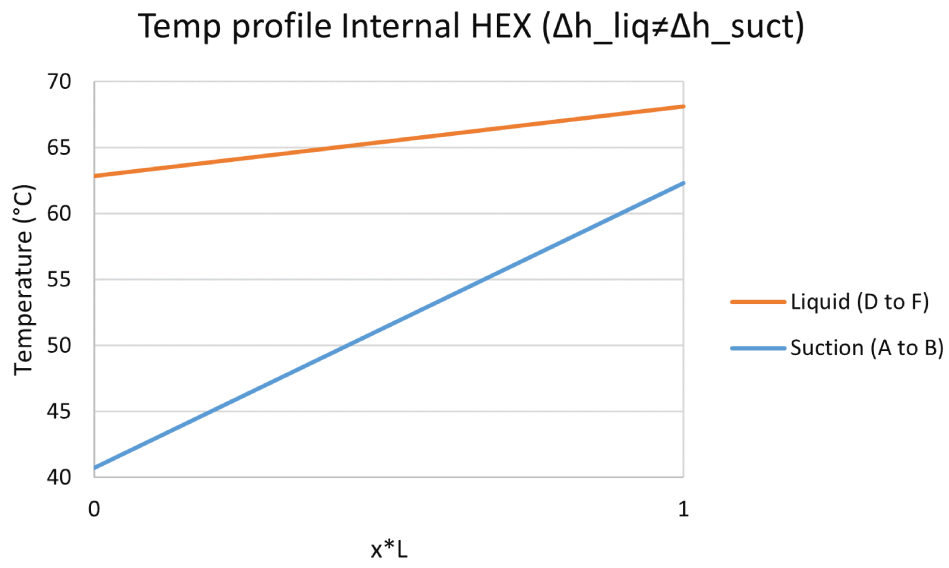


Figure B.6: Example of temperatures when sensible enthalpy is not equal for liquid/suction side.

B.2 Sanden

Figure B.7 shows the temperature profile in the condenser for one experiment with high condensation temperature and also when there is large subcooling. An example of a low UA-value resulting in a large LMTD.

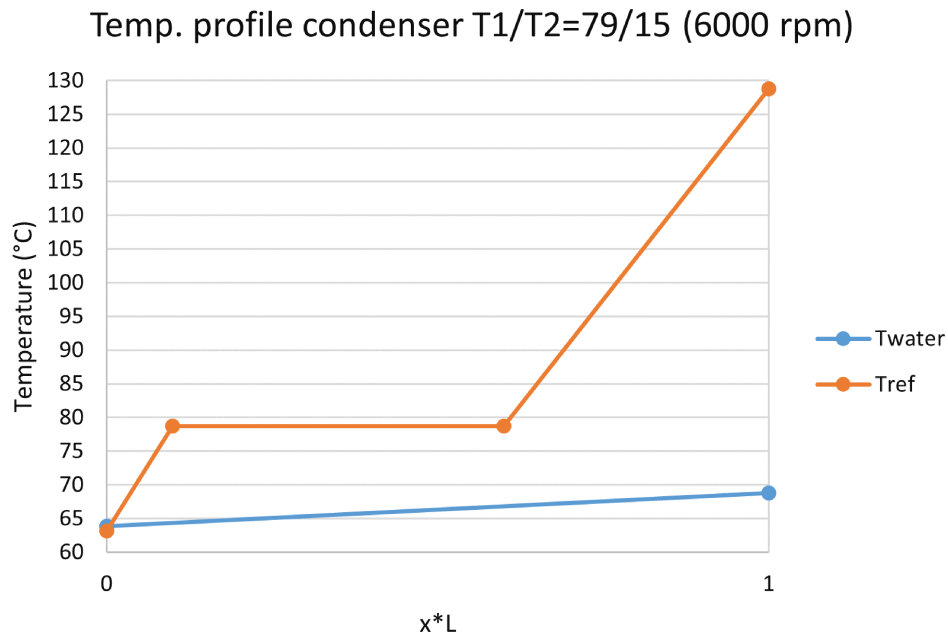


Figure B.7: Temperature profile in the condenser (length x only estimated).

Figure B.8 illustrates large temperature differences ϑ_{in} and ϑ_{out} in the evaporator.

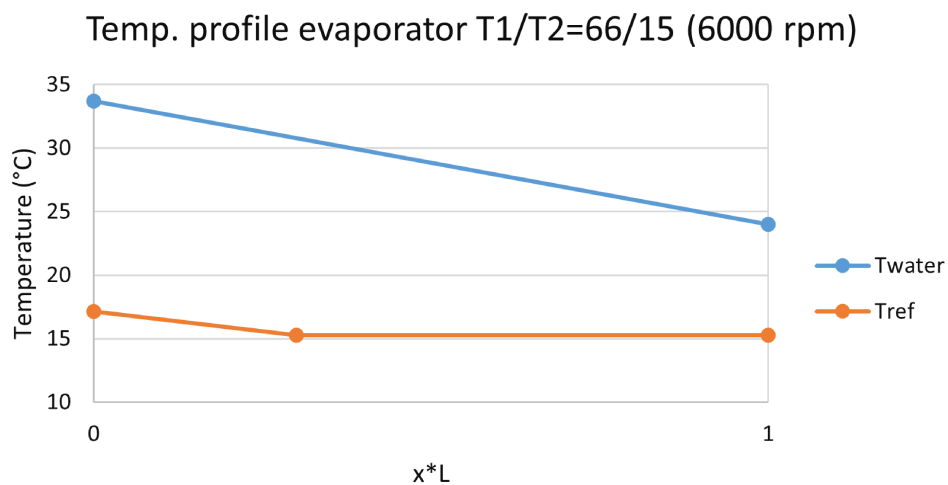


Figure B.8: Temperature profile in the evaporator (length x only estimated).

The temperature differences ϑ_{in} and ϑ_{out} in the condenser (Figure B.9) and evaporator (Figure B.10) for all experiments.

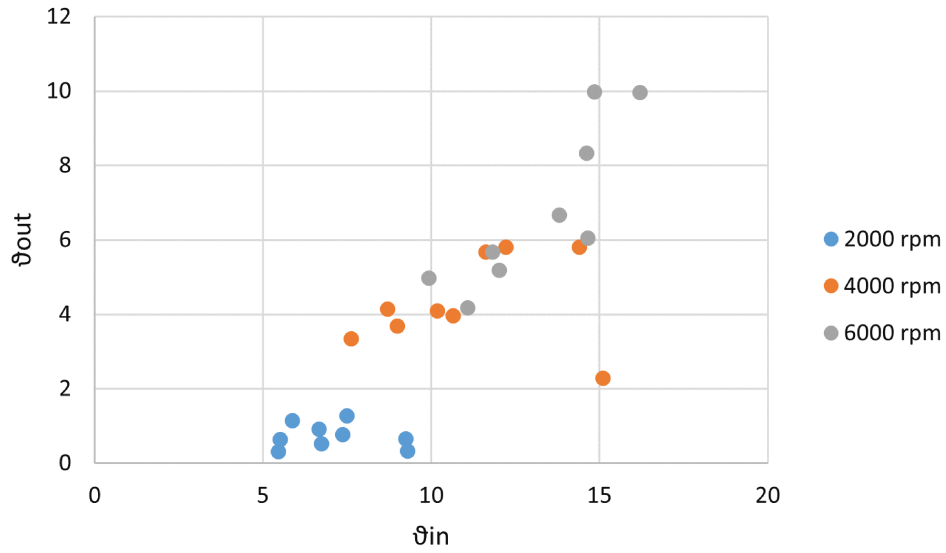


Figure B.9: Temperature differences in condenser.

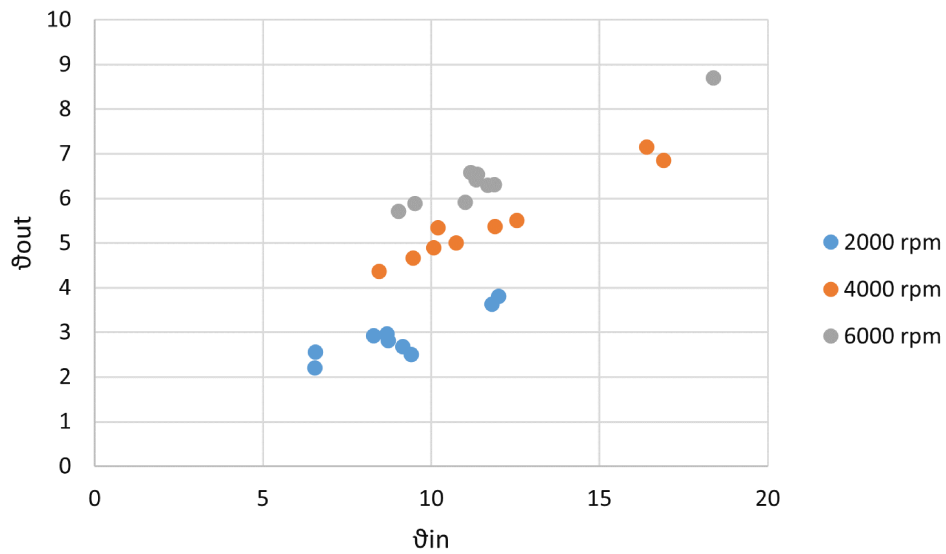


Figure B.10: Temperature differences in evaporator.

Appendix C

Temperature change with different water mass flow condenser

Figure C.1 showing condensation temperature and water temperature difference with a change in water mass flow, at a constant water outlet temperature of 60 °C. Having a low water flow seems beneficial to decrease the condensation temperature. However having a large temperature difference between incoming and outgoing water in the condenser caused problems of cooling the outgoing water in the condenser sufficiently in the experiments, especially in combination with high evaporation temperatures.

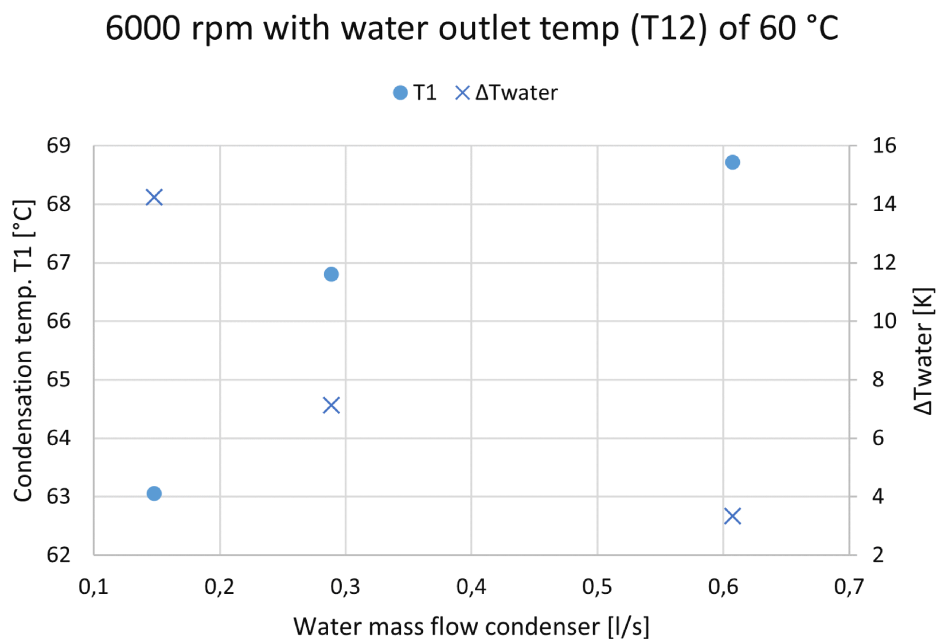


Figure C.1: Condensation temperature change with water mass flow, Sanden heat pump experiment.

Figure C.2 illustrates temperature profiles for the three different water flows.

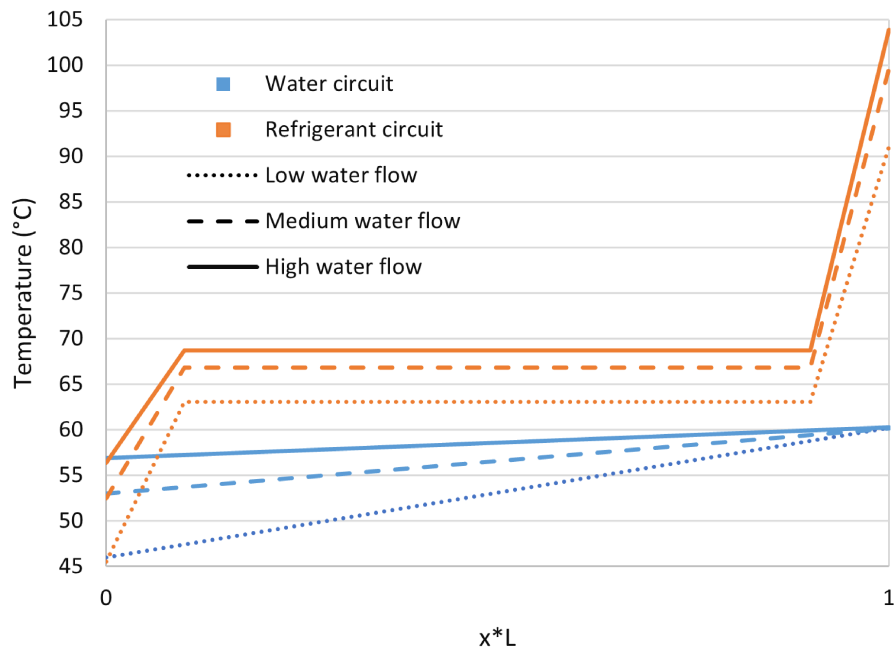
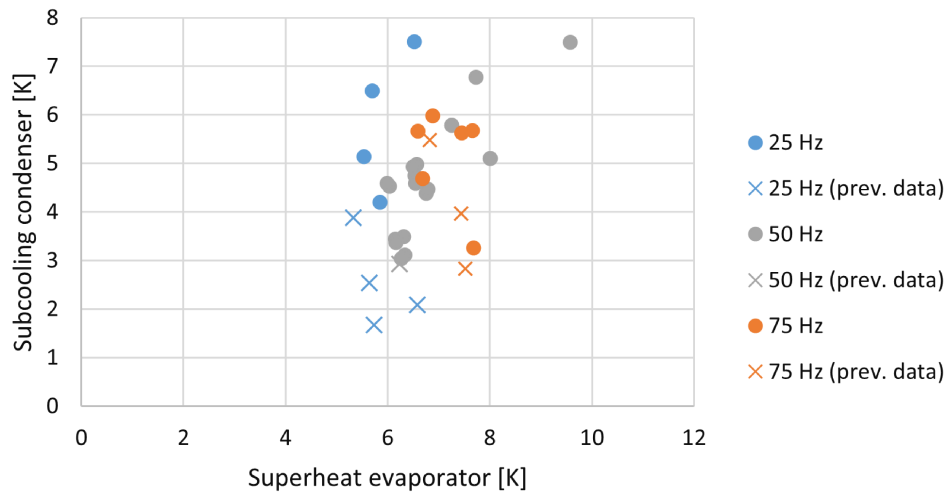


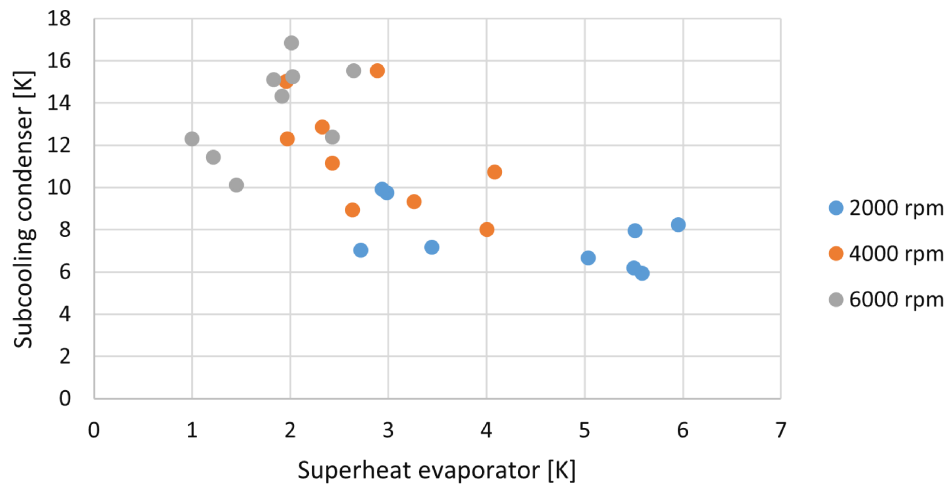
Figure C.2: Temperature profile in condenser with different water flows (length x only estimated).

Appendix D

Superheat and subcooling



(a) Bitzer heat pump.



(b) Sanden heat pump.

Figure D.1: Superheat & subcooling in experiments.

Appendix E

Heating, cooling & compressor power

	T_1/T_2	Compressor power E_k [W]	Q_1 [W]	Q_2 [W]
2000 rpm	[50/15]	426	2289	1877
	[51/25]	440	3128	2662
	[51/35]	438	4145	3637
	[60/15]	551	2226	1760
	[61/25]	565	2956	2451
	[60/35]	534	4022	3456
	[70/15]	694	2194	1608
	[70/25]	703	2864	2281
	[70/35]	680	3873	3219
4000 rpm	[53/15]	929	4650	3710
	[53/25]	984	6193	5137
	[54/35]	1055	8012	6708
	[64/15]	1131	4587	3479
	[62/25]	1146	6229	5021
	[64/35]	1261	7848	6462
	[75/15]	1337	4510	3238
	[75/25]	1425	5986	4585
	[75/35]	1514	7558	6016
6000 rpm	[54/15]	1470	6526	4996
	[56/25]	1694	8676	6882
	[55/34]	1786	10962	8665
	[66/15]	1720	6532	4832
	[67/25]	1958	8499	6472
	[66/35]	2072	10803	8607
	[79/15]	2045	6360	4387
	[79/25]	2286	8332	6083
	[77/35]	2410	10553	8058

(a) Sanden heat pump.

	$[T_1/T_2]$	Compressor Power E_k [W]	Q_1 [W]	Q_2 [W]
25 Hz	[52/35] (prev. test)	1028	10107	8731
	[49/16] (prev. test)	1144	6339	5335
	[70/16] (prev. test)	1546	5344	4055
	[70/35] (prev. test)	1685	8555	7039
	[49/2]	1047	3784	3074
	[49/13]	1130	5815	4836
	[68/2]	1232	3043	2251
	[69/14]	1495	4965	3867
50 Hz	[50/0] with frq	1982	7467	5762
	[50/11] with frq	2327	11690	9436
	[50/20] with frq	2331	14581	11894
	[60/11] with frq	2627	10674	8556
	[59/8] with frq	2465	9737	7501
	[59/17] with frq	2751	12809	10325
	[62/26] with frq	2930	16069	13095
	[70/26] with frq	3301	15407	12375
	[69/13] with frq	2927	10259	7992
	[50/11] without frq	2197	11613	9468
	[60/12] without frq	2514	11007	8668
	[61/25] without frq	2818	16021	13078
	[59/16] without frq	2617	12679	10169
	[70/13] without frq	2799	10256	7969
	[70/26] without frq	3219	15414	12341
	[61/25] (prev. test)	2834	15945	12998
	[50/0] with frq rep	1982	7467	5762
	[59/8] with frq rep	2465	9737	7501
	[68/1] with frq rep	2368	6894	4955
	[67/7] with frq rep	2604	8723	6486
75 Hz	[50/0]	3223	11475	8739
	[53/10]	3824	16026	12416
	[69/11]	4532	14850	10838
	[69/15]	4903	17327	12776
	[69/14]	4813	16264	12311
	[71/28]	5855	23325	18126
	[52/14] (prev. test)	3875	18071	14265
	[70/15] (prev. test)	4907	16970	12574
	[71/34] (prev. test)	6143	27472	21209

(b) Bitzer heat pump.

Table E.1: Heating, cooling & compressor power

TRITA TRITA-ITM-EX 2021:489